THE USE OF NARROW SPECTRAL BANDS FOR IMPROVING REMOTE SENSING ESTIMATIONS OF FRACTIONALLY ABSORBED PHOTOSYNTHETICALLY ACTIVE RADIATION (f_{apar})

by

Moon Sung Kim

Thesis submitted to the Faculty of the Graduate School
of The University of Maryland in partial fulfillment
of the requirements for the degree of
Master of Arts
1994

C.1
MD
Dept. of Geography

Advisory Committee:

Professor John R. G. Townshend, Chairman/Advisor
Professor Samuel N. Goward
Associate Research Scientist Charles L. Walthall
Adjunct Associate Professor Craig S. T. Daughtry
Adjunct Associate Professor Emmett W. Chappelle

Kim,
M. S.

ABSTRACT

Title of Thesis: THE USE OF NARROW SPECTRAL BANDS FOR IMPROVING REMOTE SENSING ESTIMATIONS OF FRACTIONALLY ABSORBED PHOTOSYNTHETICALLY ACTIVE RADIATION (f_{apar})

Name of degree candidate: Moon Sung Kim

Degree and Year: Master of Arts, 1994

Thesis directed by: Professor John R. G. Townshend,
Chairman, Department of Geography

Most remote sensing estimations of vegetation variables such as leaf area index (LAI), absorbed photosynthetically active radiation (A_{par}), and primary production are made using broad band sensors with a bandwidth of approximately 100 nm. However, high resolution spectrometers are available and have not been fully exploited for the purpose of improving estimates of vegetation variables. The study was directed to investigate the use of high spectral resolution spectroscopy for remote sensing estimates of f_{apar} in vegetation canopies in the presence of nonphotosynthetic background materials such as soil and leaf litter.

A high spectral resolution measure defined as the chlorophyll absorption ratio index (CARI) was developed for minimizing the effects of nonphotosynthetic materials in the remote estimates of f_{apar}. CARI utilizes three bands at 550, 670, and 700 nm with bandwidth of 10 nm. Simulated canopy reflectance of a range of leaf area index (LAI) were generated with the SAIL model using measurements of 42 different soil types as canopy background. CARI calculated from the simulated canopy reflectance was compared with the broad band vegetation indices such as normalized difference vegetation index (NDVI), soil adjusted vegetation index (SAVI), and simple ratio (SR). CARI reduced the effect of nonphotosynthetic background materials in the assessment of vegetation canopy f_{apar} more effectively than broad band vegetation indices.

DEDICATION

This research is dedicated to my parents June and Don, to my brother Moonjohn, to my sister Moonsue, and my lovely wife Hyern Ju.

ACKNOWLEDGEMENTS

This research was supported by the Biospheric Sciences Branch, NASA/Goddard Space Flight Center and the Remote Sensing Laboratory, USDA Beltsville Agricultural Research Center.

I am thankful to my thesis committee members for their interest and support, which included: Drs. John Townshend, Samuel Goward, Charles Walthall, Craig Daughtry, and Emmett Chappelle. Also, I would like to thank Mr. James McMurtrey for the encouragement, Mr. Frank Wood and Mr. Larry Corp for providing assistance, and Mr. Frederick Hummerich for providing the SAIL model software source code.

TABLE OF CONTENTS

TABLE OF CONTENTS(cont.)

LIST OF FIGURES

LIST OF FIGURES(cont.)

LIST OF TABLES

CHAPTER 1. REMOTE SENSING OF VEGETATIVE SURFACE

1.1 Importance of Monitoring Vegetation

1.1.1 Overview

Over the past thirty years, the advancement of space technology has allowed observation and study of the interaction between light and vegetation surface on a global scale. The objectives of global scale studies focus on the ability to predict vegetative changes that will take place in the near future and for decades to come. Global scale observations provide a new approach to the study of the Earth's ecosystems for acquiring an understanding of the evolution and functioning of the Earth's vegetation.

Global change arises in part from the result of intricate interactions of the Earth's ecosystems. The major biological component in the ecosystem is vegetation. At least 40% of the global land surface is covered by forests and woodlands that are responsible for approximately 70% of the annual net carbon accumulation (Lieth, 1975). Also, the distribution of vegetation is closely related to climate condition. This relationship between climate and the vegetation type is recognized by the names given to global vegetation zones such as tropical rain forest, boreal forest, and desert scrubs (Larsen, 1980; Woodward, 1987).

Vegetation is near the base of the food chain, and arguably, it is an essential natural resource on which humans and animals depend. Changes in plant yields and distribution will in turn affect other components of the Earth's system such as climate.

Thus, vegetation dynamics are among the most important variables governing the present and future ecological status of the Earth.

1.1.2 Absorbed Photosynthetically Active Radiation

In order to use remote sensing to monitor vegetation, an understanding of the complex radiation interactions that take place in a vegetation canopy is essential (Goel and Grier, 1988). The radiation in the wavelength region of 400 nm to 700 nm is the energy source for photosynthesis of green biomass and is defined as photosynthetically active radiation (PAR). The biomass yield reflects the efficiency of converting the radiation energy to chemical energy through photosynthesis. PAR absorption can be affected by physiological changes in the plant due to a number of stress factors such as drought, acid rain, and nutrient deficiency or other environmental factors (Asrar, 1989; Russel et al., 1989; Yoder, 1992).

A_{par} is the amount of PAR absorbed and f_{apar} is the fraction of incoming PAR absorbed by vegetation. These parameters can be used to estimate photosynthetic process, and primary production. Many studies have demonstrated that crop production is directly related to f_{apar} (Monteith, 1970; Hatfield and Carlson, 1976; Kumar and Monteith, 1981; Asrar et al., 1985; Rosenthal et al., 1985; Daughtry et al., 1992). Hatfield et al. (1983) reported that crop yield models require an estimate of either the leaf area index (LAI) or the amount of intercepted PAR (I_{par}). Similarly, PAR estimated from routine solar irradiance measurements can be used in crop growth models (Meek et. al, 1984). Venkateswarlu et al. (1987) studied the influence of A_{par}

on grain density of rice and found that the production increased as PAR increased. In summary, many studies have illustrated the importance of f_{apar} in assessing vegetation growth and yield. Thus, accurate estimations of f_{apar} are vital in evaluating ecological status due to vegetational changes.

1.2 Role of Remote Sensing

1.2.1 Background

Physical geography is an area of study that interrelates the important elements of Man's physical environment. It draws on several natural sciences for its subject matter which include science of atmosphere, ocean, earth, soils, vegetation, and landform. It also emphasizes spatial relationships such as the systematic arrangements of environmental elements into regions over the Earth's surface and the causes for those patterns. The focus of physical geography is on the life layer, a shallow zone of the lands and oceans containing most of the world of organic life, or biosphere (Strahler et al., 1978).

In recent years, major changes have taken place in the content of physical geography in part caused by the major role of the techniques of remote sensing in changing the quantity and quality of observations of the environment. Remote sensing refers to the group of techniques of collecting information about an object and its surroundings from a distance without physically contacting them. However, the term is chiefly associated with observing systems acquiring information about the land surface features from aircraft and satellite platforms.

Remote sensing systems measure reflected and emitted electromagnetic energy from surface features. The major wavelength regions used for remote sensing range from 0.4μm (visible) to 12 μm (infrared) and 30 mm to 300 mm (microwave). The significance of these wavelengths depends on the interactions of the surface features with the electromagnetic energy. Within the contexts of this thesis, review is confined to remote sensing of vegetative surface features in the wavelength region of the solar spectrum.

1.2.2 Assessment of Vegetation Variables

Since the first launch of the Landsat in 1972, a series of Earth observation satellites have provided the potential for monitoring surface materials over a large range of temporal and spatial scales. Recent advances in computing power and communication technologies have enhanced the use of remote sensing at a global scale. Remote sensing has been used to characterize not only the surface features of the globe, but also the factors related to surface features. The most important contribution of remote sensing studies of vegetated surface has been to improve our comprehension and characterization of the atmosphere-plant-soil complex.

Remote sensing studies of vegetation variables include those affecting the rate of vegetative ecosystem processes such as f_{apar}, plant production, photosynthesis, and evaportranspiration (Running et al., 1989). Also, variables that are associated with the state of the vegetation ecosystem processes include LAI, percent canopy cover, and background materials. The use of remote sensing extends to the assessment of

vegetation health or vigor and contributing factors such as environmental and natural stresses (e.g. drought, acid rain, heavy metal, nutrient deficiency).

1.3 Principal Components of Remote Sensing

In general, remote sensing as a system consists of following components: 1) radiation source, 2) radiation interactions with surface features, 3) sensing instrument, and 4) analysis and applications. This thesis is about the studies of the use of remote sensing in the quantitative assessment of a biophysical property of vegetative surface and this review concentrates on these aspects of remote sensing relevant to this topic.

1.3.1 Solar Radiation and Atmosphere

The solar radiation reaching the top Earth's atmosphere is essentially the spectrum of a black body at 6000°K modified by the absorptions of atomic gases (Fraunhofer lines) in the Sun's atmosphere (Richards, 1986; Lo, 1986).

There are three types of scattering which cause changes in intensity and direction of radiation. Scattering is wavelength dependent, in general, it decreases with increases in wavelength. Rayleigh scattering is caused by the molecules and small particles with diameters less than the wavelength of the radiation. The intensity of Rayleigh scattering is inversely proportional to the fourth power of the wavelength. The blue color of the sky on a clear day results from the effects of Rayleigh scattering in that radiation with shorter wavelengths including the ultraviolet (UV) radiation are scattered more than the radiation in the longer wavelength. Mie scattering occurs

when aerosol particles with diameters that are approximately equal in size to the wavelength of the radiation are present. Radiation at longer wavelength than in the case of Rayleigh scattering are affected by Mie scattering. Lastly, when the aerosol particles are larger than the radiation wavelength scatter is non-selective and is called non-selective scattering. This type of scattering is observed in white clouds in which water droplets scatter in all wavelengths.

In the Earth's atmosphere, solar radiation is absorbed by gases such as ozone (O_3), oxygen (O_2), carbon dioxide (CO_2), and water (H_2O). As a result of this absorption, solar radiation is attenuated or lost. The transmission properties of the atmosphere is important in determining the wavebands which can be sensed by an airborne or satellite platform. Between main zones of atmosphere absorption there are certain 'spectral windows' that are used in remote sensing of the Earth' surface. The principal atmospheric windows include the visible portion of the spectrum (i.e., 0.30-0.75 μm), near infrared (i.e., 0.77-0.91 μm, 1.0-1.12 μm, 1.19-1.34 μm, 1.55-1.75 μm, and 2.05-2.4 μm) portion of the spectrum, and the thermal region (8.0-11.0 μm).

Figure 1.1 illustrates the spectral distribution of solar radiation at sea level and at the top of the Earth's atmosphere. The irradiance values were derived from LOWTRAN6 software. The differences in the spectra are the results of the atmospheric scattering and absorption. The largest differences between these spectra in the UV region are the effects of Rayleigh scattering. Sharp absorption peaks due to the atmospheric gases are seen in the near infra-red (IR) region and broad water absorption wells are visible in the mid-IR region.

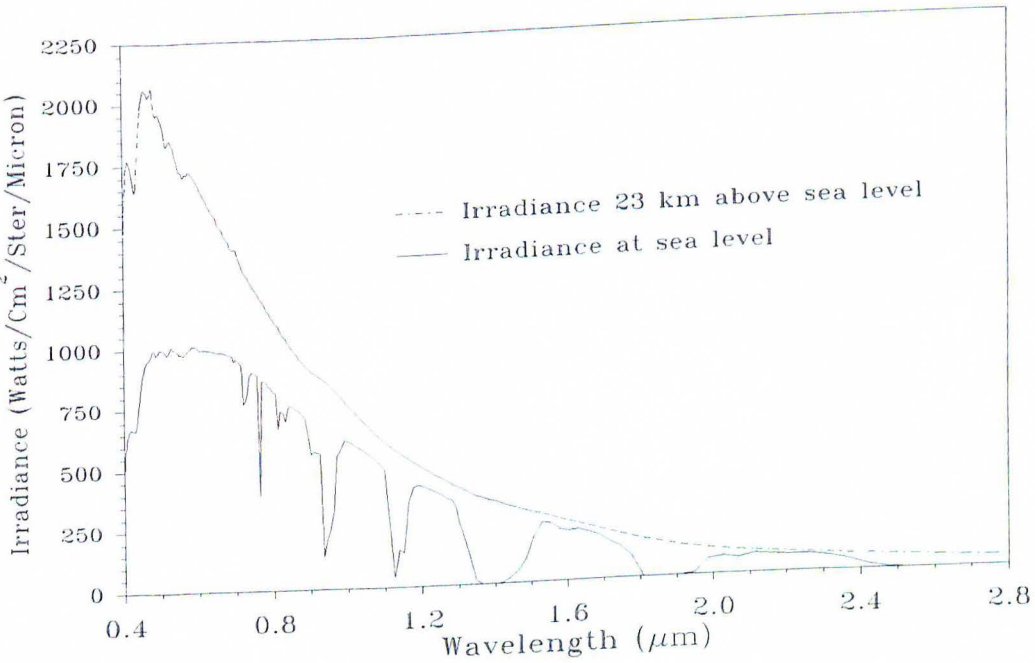

Figure 1.1 Solar irradiance received at sea level and 23 km above sea level (Redrawn from Williams, 1989).

1.3.2 Radiation Interaction with Vegetation

Single Leaf - The solar radiation incident on a leaf is either reflected, absorbed, or transmitted and is wavelength dependent. This can be expressed as follows:

$$I_\lambda = \rho_\lambda + \alpha_\lambda + \tau_\lambda,$$

where I is incident radiation, ρ_λ is reflectance, α_λ is absorption, and τ_λ is transmittance at wavelength λ (Williams, 1989). A small portion (3%) of the energy is re-emitted as fluorescence at a longer wavelength. The result of scattering within

a leaf is such that the direction of radiation is randomized. Thus, about an equal amount of light being reflected is transmitted. This accounts for close correlation between reflectance and transmittance (i.e., $\rho_{\lambda} \approx \tau_{\lambda}$). The importance of this relation is that remote sensing measurements of reflectance have been found applicable to the studies of vegetative variables, such as f_{apar}, crop yield and photosynthesis, which depend on radiation absorption (Monteith, 1970; Hatfield and Carlson, 1976; Kumar and Monteith, 1981; Sellers, 1985; Asrar et al., 1985; Rosenthal et al., 1985; Daughtry et al., 1992).

The characteristic features of leaf level reflectance and transmittance are distinctive in three spectral regions. In the VIS (visible: 0.4 μm - 0.7 μm) region, the dominant factors controlling the reflectance are the contributions of photosynthetic pigments such as chlorophylls a, b, and carotenoids. Most of the incident light is absorbed in this region. The reflectance and transmittance characteristics of the NIR (near IR: 0.7 μm - 1.3 μm) region are attributes of leaf structural components. High reflectance and transmittance in the NIR region are due to very low absorption and light scattering in the intercellular air space (mesophyll layer). In this spectral range, both reflectance and transmittance account for approximately 90% to 95% of the incident radiation. In the mid-IR (middle Infra-Red: 1.3 μm - 2.5 μm) range, dominating spectral characteristics are mainly water absorption, which occurs at around 1.4 μm and 2.2 μm. In the red-NIR region (0.68 μm - 0.74 μm), also known as the "Red Edge area" (Gates et al., 1965; Collins et al., 1983; Horler et al., 1983a), is where a transition of light interaction takes place between the leaf pigment absorption

and structural scattering.

Plant Canopy - The solar radiation reaching the top layer of a vegetation canopy is, as in the case of a single leaf, either reflected, absorbed, or transmitted. But, the reflectance properties of a single leaf are inadequate to characterize a vegetation canopy, whose reflectance is an integrated function of leaf optical properties, plant structure, reflectance of background materials, illumination zenith and azimuth angles, and sensor view angles (Colwell, 1974; Goward et al, 1992). One of the canopy reflectance characteristics that directly governs the amount of light absorption and reflectance is the quantity of photosynthetic pigments in the plant leaves. Also, the amount of exposed nonphotosynthetic materials including soil, leaf litter, and woody biomass, such as twigs, stems, and trunks have been shown to be important factors in the remote sensing assessment of vegetative variables (Choudhury, 1987; Huete, 1988; Baret et al., 1991; Goward et al., 1992).

The methods used to acquire canopy reflectance differ from the measurement method for the leaf reflectance. On a single leaf, mainly a hemispherical reflectance is measured. However, canopy reflectance is measured as a bidirectional reflectance. When measuring bidirectional reflectance of a vegetation canopy, the effects of increasing red (0.60 μm - 0.70 μm) reflectance and decreasing NIR reflectance are associated with; 1) decreasing LAI; 2) decreasing solar zenith angle; and 3) changing leaf orientation from horizontal to vertical (Suits et al., 1972; Colwell, 1974).

1.3.3 Instruments

Remote sensing instruments record reflected or emitted radiation from surface features. There are photographic and electro-optical instruments. Both systems consist of four (functionally equivalent) component parts, namely, optics, a filter or spectrometer, a recording device, and a storage device. Optics are used for collimating and focusing the radiation, and determine the field of view (FOV) and instantaneous field of view (IFOV: spatial resolution or ground resolution) of the instrument. In the case of a broad band (waveband width $\approx$ 100 nm) system, a filter is used to determine the waveband transmitted to the recording device. In a high spectral resolution or narrow band (waveband width $\leq$ 10 nm) system, a grating disperses radiation into narrower spectral regions onto detectors.

The detector records the intensity of the radiation transmitted through the filter component. In a photographic instrument, films are used as the recording and storage device. Electro-optical detectors transform radiation into an electrical signal. Depending on the physical process by which the radiation is converted to an electrical signal, there are quantum and thermal detectors. The recent development of linear array detectors and CCD (Charge coupled device) allows the possibility of high spectral resolution remote sensing. In electro-optical system, the detector output is converted to digital format and stored in a storage device (e.g. magnetic media). The advantage of digital storage is that data can be processed and produced in a quantitative form.

Figure 1.2 presents the differences between spectral reflectance of vegetation

canopy acquired with a high spectral resolution Spectron Engineering spectroradiometer (SE590) and a broad band Barnes Multiband Modular Radiometer (MMR). As seen in the figure, the narrow band reflectance depicts detailed differences (absorption characteristic of plant photosynthetic pigments) in the PAR region, which is not seen in the spectra obtained with the broad band MMR.

Current satellite sensors being used in quantitative remote sensing are broad band electro-optical scanner systems. High spectral resolution sensors such as ASAS (Advance Solid-State Array Spectroradiometer) and AVIRIS (Advanced Visible Infra-

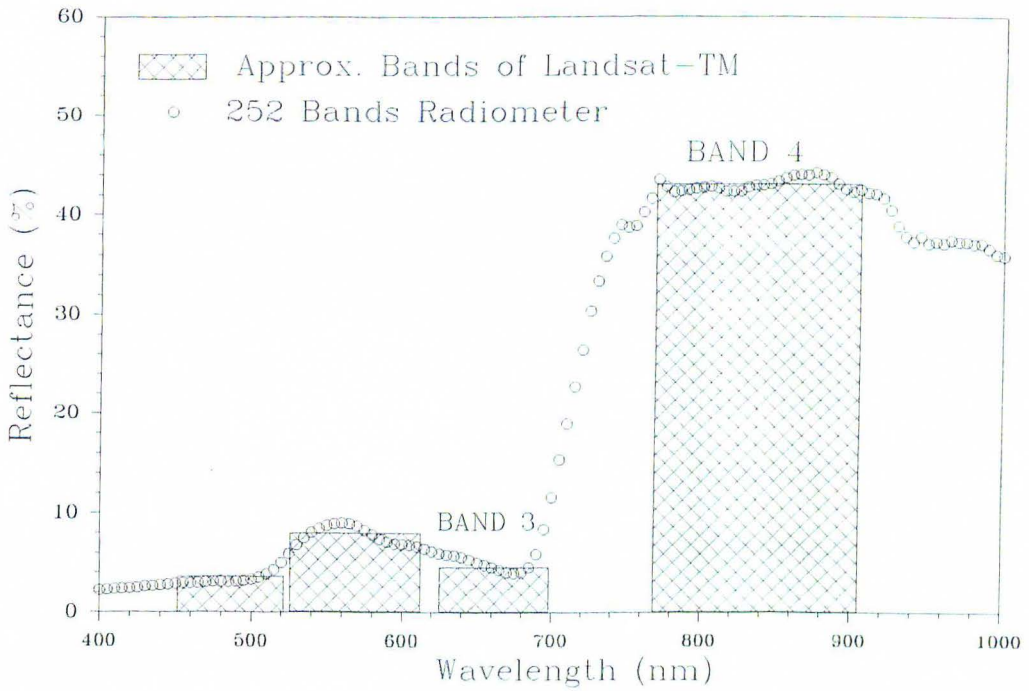

Figure 1.2 Comparison of high spectral resolution and broad band (MMR) reflectances of spruce canopy.

Red Imaging Spectrometer) are available on airborne platforms, and one of the EOS (Earth Observing System) satellite platforms in the near future has been planned to includes the high spectral resolution MODIS-T and N (Moderate Resolution Imaging Spectrometer Tilt and Nadir).

Satellites - Two types of satellites are in common use, polar orbiting (low altitude: 700-1500 km) and geosynchronous (stationary high altitude: 36000 km). Remote sensing satellites used for the quantitative assessment of vegetation variables are all polar orbiting such as the NOAA Advanced Very High Resolution Radiometer (AVHRR), the Landsat Multispectral Scanner System (MSS) and Thematic Mapper (TM), and the H-R-V of SPOT (Systeme Probatoire d'Observation de la Terre). These satellites have 5 to 7 broad band channels with spectral resolution of approximately 100 nm. The spatial resolutions of these sensors vary and are approximately 1.1 km for the AVHRR, 80 m for the MSS, 30 m for the TM, and 20 m for the SPOT.

1.3.4 Data Analysis and Applications

The type of data obtained from a remote sensing instrument is determined by such parameters as spectral range and resolution, spatial and temporal resolution, and radiometric sensitivity. When satellite-borne or airborne sensors record data radiometric and geometric distortions can occur. There are potentially many sources of errors or distortions associated with remotely sensed data. The main causes for the radiometric errors are the atmospheric effects (i.e., absorption and scattering). Sources

for the geometric distortions are associated with many factors such as; 1) rotation and curvature of the Earth; 2) variations in sensor altitude and attitude; 3) panoramic effects; and 4) aspect ratio difference. The first step involved in data analysis is data preprocessing, which is a group of procedures applied to raw data to correct for the radiometric and geometric distortions. This is followed by main processing of data for feature extraction and quantitative analysis which depend on spatial, spectral, and temporal features.

Classification - There are two types of classification methods used to characterize surface features (i.e., water, soil, and vegetation) from image data. For supervised classification, training sets which are sub-samples from the image whose feature is known are selected. These training sets are used to determine unknown areas. The statistical method called discriminant analysis is commonly employed in supervised classification. Unsupervised classification is another method in which no pre-determined training sets are used. Characterization and identification of the features are carried out by cluster analysis method which identifies groupings of patterns. The nature of each pattern is identified by field checks.

Quantitative analysis - Numerous vegetation indices (VI) have been developed to reduce spectral data to assess vegetation variables. The use of VIs were introduced on the bases of ratio and the linear combination of the Landsat MSS data. These indices exploit differences in the reflected spectral characteristics of one solar spectrum region

to another region (e.g. red and NIR). Functional manipulation of the spectral bands lead to many forms of VIs. More detailed descriptions and applications of VIs are discussed in the next section.

1.4. Current (Broad Spectral band) Remote Sensing Approach

1.4.1 Introduction

Measurements of reflected and emitted electromagnetic energy in solar spectrum serve as methods of remote sensing. Remote sensing scientists have participated in developing numerous analytical and quantitative techniques to understand ecosystem processes from remotely sensed data. The discussion in the section primarily consists of the use broad band vegetation indices (VIs) to detect or predict vegetative variables. In association with these VIs, measurements in various regions of the solar spectrum at leaf level, canopy level, and by satellite are included.

1.4.2 Application of Broad Band Vegetation Indices

VIs exploit the differences in spectral interactions of vegetation mostly in the red and the NIR regions. Commonly, VIs are formulated as the differences divided by the sum (normalized differences) or ratio of two bands. The most frequently used VIs are the NDVI (Normalized Difference Vegetation Index) of Rouse et al., (1974) and SR (Simple Ratio) where the NDVI is calculated as (NIR - red) / (NIR + red) and SR is calculated as (NIR / red). Both theoretically and experimentally, these VIs have been demonstrated to be related to f_{apar}, LAI, and fraction of vegetation cover

(Tucker, 1979; Kumar and Monteith, 1981; Jackson, 1983; Sellers, 1985; Asrar et al., 1985; Daughtry et al., 1992).

Dusek et al., (1985) presented 1240 vegetation indices calculated from the seven reflectance bands (3 visible bands and 4 NIR bands) of the Barnes MMR which simulates the bands of the Landsat-5 TM bands. These indices consisted of individual bands, various band ratios, ratios of differences divided by sums (normalized difference), and linear combinations (N-space). The five growth parameters, LAI, green ground cover, total wet and total dry phytomass, and green leaf phytomass were measured approximately monthly along with spectral reflectance data until spring regrowth began. The results indicated that the indices were linearly related to the plant parameters and could be used as a simple method for estimating the plant parameter desired.

Studies by Tucker et al., (1981) showed significant relationships between total above ground dry-matter accumulation in winter wheat and the NDVI and SR. The NDVI and SR plotted against Julian date showed the effect of increasing chlorophyll absorption until the onset of senescence which resulted in progressively higher levels of reflected radiance. Paltridge et al., (1988) reported a modified NDVI from NOAA, AVHRR data to monitor grassland dryness and fire potential in Australia. It was calculated as slightly modified NDVI; V = (NIR - 1.2 X red) / (NIR + red), where the value 1.2 is derived from the NIR and red radiance ratio (NIR/red). This ratio converged to 1.2 as vegetation dried out. The modified vegetation index value for dry vegetation is zero and maximized the contrast in "greenness". Another modified NDVI

reported by Chorowicz et al., (1990) utilized the Landsat TM band 7 to enhanced and maximized the effects of illumination geometry. The VEGTM7 was calculated as (TM7 - VEG) / (TM7 + VEG), where VEG = NDVI = (TM4 - TM3) / (TM4 + TM3).

The effects of the different wavelength bands on the NDVI and SR were tested based on the data simulated for the Landsat-5 MSS and TM, NOAA-9 AVHRR, and SPOT-1 sensor systems in relationship to agronomic ground measurements (Gallo et al., 1987). This study reported that although these sensors have different wavebands, the vegetation indices calculated from the four systems were associated with similar amounts of variations in the agronomic measurements.

1.4.3 Limitations of Broad Band VIs

Studies in the regions of VIS and NIR have been carried out most vigorously and numerous forms of variations of VIs has been derived. Also, the relationships between these VIs and vegetation parameters have been reported. However, most of these various VIs are functionally equivalent among each other (Perry et al., 1984; Baret et al., 1991). Investigations by Perry et al., (1984) demonstrated functional equivalence of spectral VIs presenting the origin, derivation, and other factors. These investigations summarized the variations among many forms of vegetation index formulae and the empirical relationships among them and illustrated the idea of some vegetation indices being functionally equivalent for decision-making. This was examined with two false color images of the same scene generated with the NDVI and

SR. From this comparison, the study concluded that although the two images looked different, the difference resulted from the color assignment intervals rather than from the VI used. In conclusion, the paper argued that most vegetation index formulae fall into two categories, either using ratios or using differences to exploit the spectral characteristics of soil and vegetation.

Many studies have shown the relationships between remotely sensed reflectance of vegetated surfaces and f_{apar}, but the estimations were exclusively based on the broad band VIS-NIR vegetation reflectance indices (Asrar et al., 1985; Choudhury, 1987; Daughtry et al., 1992). The variables contributing to a vegetation canopy reflectance are leaf optical properties, plant structure, illumination and view angles, and soil background where variations of these canopy variables have been shown to affect the remote sensing estimations of f_{apar}. Specifically, the relationships between the broad band reflectance vegetation indices and f_{apar} were very sensitive to variations in the reflectance of nonphotosynthetic background materials (Choudhury, 1987; Huete, 1988; Baret et al., 1991; Goward et al., 1992).

1.4.4 Effect of Soil Background

Soil background influence is most apparent with incomplete canopy closure. Soil reflectance variations result from moisture, roughness, shadow, and organic matter differences are reported (Huete, 1988). For a given amount of vegetation darker soil background reflectance resulted in higher values in the NDVI and SR (Colwell, 1974; Huete, 1985). On the contrary, an opposite soil effect was reported on the PVI

(Perpendicular Vegetation Index: Richardson and Wiegand, 1977) by Huete, (1985).

The sensitivity of the VIs varies to soil background materials have been manifested by the modification applied to the NDVI to eliminate the soil reflectance effects in a vegetation canopy. Choudhury (1987) reported that the vegetation-soil relationship could be parameterized at the local size scale by NDVI = NDVIO + (NDVIM - NDVIO) x $(1 - e^{-ha})$, where a is an indicator of chlorophyll content such as LAI, h is the NIR transmisivity, and NDVIO and NDVIM are, the values of NDVI for bare soil and full vegetation cover, respectively.

Variations of the VIs have been reported to enhance the characterization of soil background reflectance in vegetation canopy reflectance. These VIs rely on the "soil line" in red and NIR soil reflectances plotted in red-NIR wavelength space (soil line = NIR - a· red, where a is the slope of the soil line). The PVI (Richardson et al., 1977) was one of the first VIs reported to reduce soil background influence and was calculated as $1 / (a^2 + 1)^{1/2}$ X (NIR - a·red - b).

The SAVI (Soil Adjusted Vegetation Index) uses a transformation technique to minimize soil brightness influences from spectral vegetation indices involving red and NIR wavelengths (Huete, 1988, 1989). The SAVI was calculated as [(NIR - red) / (NIR + red + L)] X (1 + L), where L is a soil isoline factor that involved a shifting of the origin of reflectance spectra plotted in NIR-red wavelength space to account for first-order soil-vegetation interactions, and differential red and NIR extinction through vegetation canopy. It was noted that there may actually be two or three optimal adjustment factors depending on the vegetation densities (e.g. low: L=1, intermediate:

L=0.5, and high: L=0.25). The study concluded that for any adjustment factors from 0.25 to 1 the soil influences were considerably reduced in comparison to the NDVI and PVI.

Baret et al. (1989, 1991) reported the TSAVI (Transformed Soil Adjusted Vegetation Index) and is given by:

$$TSAVI = a \cdot (NIR - a \cdot red - b) / [a \cdot NIR + red - ab + X \cdot (1 + a^2)] ,$$

where a and b are the parameters of the soil line and X value of 0.08 was suggested to minimize soil effects. They reported the comparative studies between the VIs devised to minimize soil effects. The studies concluded that the PVI, SAVI, and TSAVI were effective in lower LAI ranges (LAI < 2-3), but, indicated ineffectiveness for higher LAIs.

1.5 High Spectral Resolution Approach

The use of high spectral resolution spectroscopy has until recently been confined to laboratories and its main use was to characterize the spectral properties of individual leaves (Gates et al., 1965). One of the early remote sensing application of high resolution spectroscopy measurements was the use of a single narrow band to assess leaf pigment concentrations (Harwick et al., 1975; Tucker et al., 1975). More recent studies by Yoder et al., (1990) and Chappelle et al., (1992) aimed at non-destructive estimates of leaf pigment concentrations demonstrated successful use of more than a single narrow reflectance band.

The ratio analysis of reflectance spectra (RARS) by Chappelle et al., (1992)

showed that ratios of narrow reflectance bands correlated highly with leaf pigment concentration and could be used in remote assessment of A_{par}. The RARS algorithm utilizes reflectance values at 500 nm, 550 nm, 650 nm, 670 nm, 700 nm, and 760 nm. More specifically, ratios of 675 nm / 700 nm, 675 nm / (650 nm X 700 nm), and 760 nm / 500 nm were empirically derived to estimate concentrations of chlorophyll a, chlorophyll b, and carotenoids, respectively.

Advancement of sensor technology and availability of field-portable high resolution radiometers have extended the use of high resolution reflectance data in the remote sensing applications. Leckie et al., (1988) conducted ground-based spectral reflectance measurements of a single crown of balsam fir trees with varying degrees of defoliation caused by feeding of the spruce budworm. They used four estimates of defoliation symptoms (i.e., percent needles, percent bare twigs, percent feeding debris, photo visual redness) where each symptom was defined as healthy, light, moderate, and severe level. The reflectance measurements were related to damage symptom quantity to identify good wavelengths for discriminating different levels of damage symptoms. They noted that narrow, well-placed spectral bands were important for defoliation assessment.

Williams (1989) studied optical-reflective radiative transfer characteristics of spruce and conifer species at the needle, branch, and canopy levels in association with cold climate and short growing seasons. This research included high spectral resolution canopy reflectance measurements from a helicopter platform. The use of high spectral resolution airborne sensor systems was also reported by Wessman et al.,

(1988) in the assessment of foliar chemistry.

The red edge of the reflectance spectrum is defined as the rising slope of the reflectance spectra in the red-NIR region. The red edge shift is detected by the position of the inflection point of the first derivative of the reflectance spectra. It was first noted by Gates et al., (1965) that as the concentration of chlorophyll increased, the red edge shifted toward longer wavelengths. Collins et al., (1978, 1983) reported similar shifts in the red edge of the wheat reflectance measurements obtained from an aircraft using a high spectral resolution spectroradiometer. An increasing shift toward longer wavelengths was observed as the crop matured, and they speculated the shift was due to an increase in the chlorophyll concentrations.

Rock et al., (1988) observed the red edge shift of 5 nm from reflectance measurement of red spruce (Vermont) and Norway spruce (Baden-Wurttemberg, Germany) in accordance with the canopy damage levels. Other investigations have reported that the red edge shift toward shorter wavelength was observed in vegetation that had been growing in soils with heavy metal content (Horler et al., 1980; Collins et al., 1983; Goetz et al., 1983) and in vegetation subjected to environmental stress such as "acid rain" (Rock et al., 1986).

Only a few researchers to this time have worked with narrow band spectral reflectance as a mean of eliminating the effects of nonphotosynthetic background materials in vegetation canopy reflectance. Recent studies demonstrated that remote sensing application of high resolution spectroscopy techniques could reduce the effects of soil background reflectance in vegetation canopies (Hall et al., 1990; Demetriades-

Shah et al., 1990). These studies employed first and second derivative analyses methods that are commonly used in analytical chemistry for the elimination of background signals.

1.6 Research Objectives

1.6.1 Rationale for the Use of Narrow Band Reflectance

The goal of the quantitative ecosystem remote sensing is to assess electromagnetic energy interactions to derive the most accurate information about vegetative variables. The light interaction through the atmosphere-canopy is a complex mechanism and insufficient understanding of the spectral characteristics of the complex features extends opportunity for new approaches. Current remote sensing estimates of vegetation variables such as LAI, f_{apar} ,and crop yield are exclusively based on the broad band VIs with bandwidths of approximately 100 nm. It has been shown that these remotely derived estimates vary as a result of spectral variability of background materials (Choudhury, 1987; Huete, 1988; Baret et al., 1991; Goward et al., 1992).

Recent advances in technology allowed us to apply high spectral resolution spectroscopy in remote sensing (Williams, 1989), but it has been little explored for the purpose of characterization of vegetation-soil complex. Although as the previous section showed some limited studies have been carried out, little or no exploration has been made of the use of narrow band sensing for deriving vegetation indices. Many of the studies that have been made show that many forms of broad band vegetation indices are variations of and functionally equivalent to the NDVI and SR (Perry et al.,

1984; Baret et al., 1991). Many bands are available with high spectral resolution sensing. This gives rise to the following question: Is it possible to extract more accurate information from narrow reflectance bands than broad reflectance bands? The research which was conducted was an attempt to answer this question.

1.6.2 Objective Statements

The main objectives of this research is to investigate the use of narrow band reflectance and develop a method for estimating vegetation canopy f_{apar}. This research concentrated on reducing the variability in the f_{apar} estimates due to the presence of diverse nonphotosynthetic materials, such as soils and leaf litter.

Canopy reflectance is determined by complex interactions of leaf optical properties, background reflectance, atmosphere, solar illumination angle, and sensor view angle. It is of interest to consider the contributions of all these factors contributing to canopy reflectance. Nevertheless, it is an extremely complicated process and is beyond the scope of this research. This research was rather confined to and focused on to reduce the effects of reflectance and scattering due to nonphotosynthetic background material to better estimate f_{apar}.

CHAPTER 2. EXPERIMENTAL SET UP AND DATA ACQUISITION

2.1 Introduction

The main objective of this research is to investigate the use of narrow reflectance bands in remote estimates of canopy f_{apar}. The research concentrated on reducing the variability in the f_{apar} estimates due to the presence of diverse nonphotosynthetic materials. This research utilized narrow spectral bands with bandwidth of approximately 10 nm.

The investigation was conducted on the dicot, soybean (Glycine max L.). Soybean plants were grown in the greenhouse at Beltsville Agricultural Research Center (BARC) of the United States Department of Agriculture (USDA) in Beltsville, Maryland. Spectral data sets including leaf level reflectance and soil reflectance were measured. In conjunction with the spectral data set, pigment concentration of the leaf samples used for the reflectance measurements were obtained. Canopy level reflectance were acquired using a radiative transfer model.

2.1.1 Model Simulated Canopy Reflectance

In recent years considerable effort has been directed towards the development of canopy reflectance models. These models have provided tools to: 1) assess the effect of different canopy characteristics on reflectance; 2) evaluate plant canopy reflectance under varying observation conditions; and 3) explore relationships between biophysical properties (i.e., LAI, f_{apar}) and canopy reflectance (Suits, 1972; Kimes et

al., 1984; Verhoef, 1984). One of the simplest canopy reflectance models is the Suits model (Suits, 1972) in which a vegetative canopy is assumed as segments of vertical and horizontal components. The SAIL (scattering from arbitrarily inclined leaves; Verhoef, 1984; Badhwar et al., 1985) model, a modified version of the Suits model, incorporates leaf distribution angles. Thus, it simulates more realistic canopy reflectance.

For evaluating the proposed narrow band method, the SAIL model was used: 1) to simulate soybean canopy reflectance as a mixture of green biomass and background material components; and 2) to derive f_{apar}. This model has been used successfully in applications similar to the present one (Hall et al., 1990; Goward et al., 1992).

2.2 Experimental Procedures

An experimental strategy was devised to empirically develop a narrow band method to determine canopy level f_{apar} (Fig. 2.1). The strategy had three stages. In the first stage, the soybean leaf reflectance measurements and pigment concentration data were used to develop a narrow band vegetation greenness index. The leaf reflectance in the VIS is mainly governed by the amount of the plant pigments. By utilizing the absorption characteristics of these pigments in the leaf level reflectance allowed the development of a greenness index which reduces the effects of background materials and only depicts the absorption characteristics of these pigments.

When background reflectance components (such as soils) were introduced to

the narrow band greenness index the characteristics of this index in relation to PAR absorption (f_{apar}) were speculated to be affected. The second stage of the research consisted of validation and modification of the use of this greenness index in the canopy level reflectances which were simulated by the SAIL model. Various soil background reflectances were used as the canopy background and very low to high LAI were simulated to cover a range of canopy conditions.

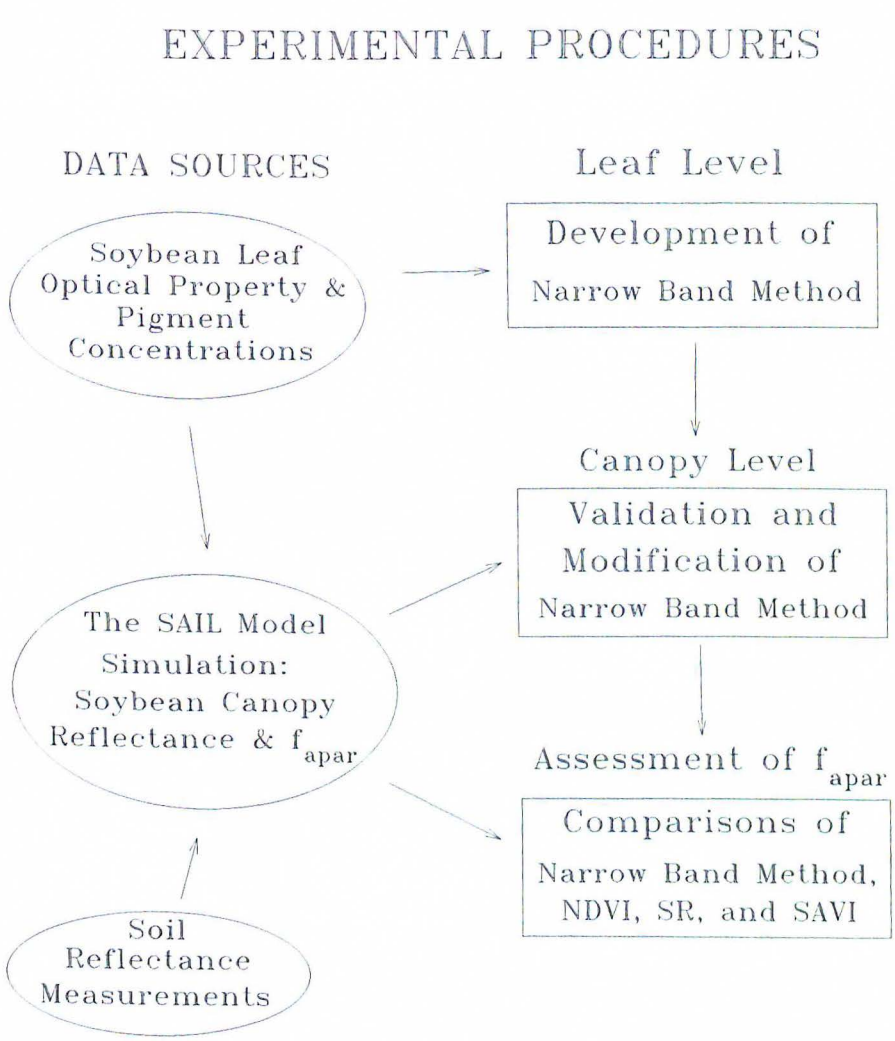

Figure 2.1 Diagram of experimental procedures

Finally, the narrow band method was evaluated by comparing it to broad band VIs, such as the NDVI, SR, and SAVI. These broad band VIs were also calculated using the simulated canopy reflectance from the SAIL model .

2.3 Measurements

2.3.1 Leaf Level Reflectance

Greenhouse grown soybean leaves were used for the leaf level reflectance measurements. The plants were grown in perlite for six weeks at five different nitrogen (N) levels with urea as the nitrogen source. The nutrient solutions contained, along with the other essential nutrients optimal for soybean growth, urea at concentrations of 4×10^{-3} moles/l, 2×10^{-3} moles/l, 1×10^{-3} moles/l, 5×10^{-4} moles/l, and 0 moles/l. These five groups of soybeans (ten plants per group) were 100%, 50%, 25%, 12.5%, and 0% of the amount of N required for optimal growth rate, respectively. The plants were watered daily, and the nutrient solutions were given twice a week. These varying N concentrations produced a range of N deficiency stress that resulted in a range of leaf pigment concentrations and a range of reflectance spectra.

Leaf reflectances were acquired with a LI-COR 1800 integrating sphere spectroradiometer (LI-COR, Inc. of Lincoln, Nebraska). The instrument has a spectral range of 300 nm to 1100 nm with a spectral resolution of 6 nm. The LI-COR integrating sphere is a "closed system" which allows quantification of total radiation reflected from (or transmitted through) a sample from a light source illuminating the

surface from a single direction. Thus, the system measures hemispherical reflectance factors. The system consists of a hollow aluminum sphere (7.5 cm diameter) that is internally coated with barium sulfate, a 10-W tungsten-halogen light source with optics, and a radiometer unit with a fiber optic cable attachment.

The sphere has four ports where the light source, fiber optic cable to the detector unit, a reference material, and a sample are placed (figure 2.2). The light source is held at the opposite side of the sample port where the optics focus the illuminating beam onto the sample within the sample port. A third port holds the fiber optic cable where the radiation inside the sphere is transmitted to the spectrometer. The fiber optic's field of view (FOV) is directed away from the sample port to the

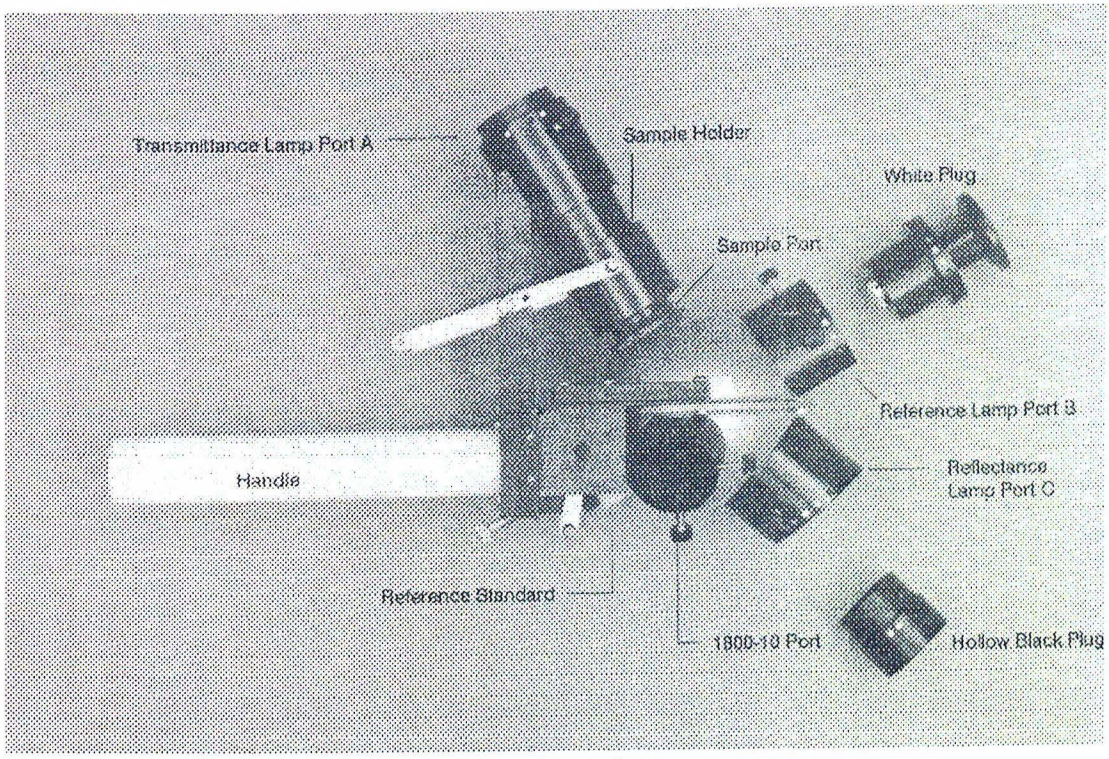

Figure 2.2 Parts of LI-COR integrating sphere.

sphere wall. This arrangement allows to acquire the reflected and scattered radiation from the sample uniformly illuminated onto the sphere wall.

The radiometer unit contains a microprocessor and a PC interface where data can be internally stored or transferred to a computer for later processing and analysis. The data acquisition sequence is such that radiation via fiber optic attachment is detected by a silicon photodiode detector, analogue signals from the detector are converted to digital signals, and then the digital signals are stored in the microprocessor as a binary formatted file. Data transfer software was provided by LI-COR, Inc. The binary format was converted to ASCII format when transferred to a PC. The ASCII format files were processed by PC-based software that was developed by the author to calculate percent reflectance.

In order to derive the reflectance factor, reflected and scattered radiation from the reference surface is divided into reflected and scattered radiation from a sample (e.g. a leaf). More detailed descriptions to calculate the leaf optical properties using the sphere system were reported by Daughtry et al., (1989). The reference surface was pressed barium sulfate powder. The reference surface was mounted on one of the ports and was used for all the leaf samples. Thus, the surface of the reference material became a part of the sphere wall along with the sample. To determine the radiance due to the reference surface, the lamp was moved to another port to illuminate the reference surface while the sample was still mounted on the sample port.

A total of 50 pairs of scans (50 reference and 50 samples) of 10 leaves from each nitrogen treatment group were acquired at 5 nm intervals from 400 nm to 800 nm

on a 2.5 cm^2 circular target area. The leaves were excised immediately before scanning from the upper most fully expanded trifolia. Spectra in terms of percent reflectance were obtained by dividing the reflected radiation from the samples by the reflected radiation by the reference, and then multiplying by 100 (Eq. 2.1). Stray light (ambient radiation in the system), measured without any sample on the sample port, was subtracted from the sample and reference measurements.

$$\text{Percent Reflectance}_{\lambda} = (\tau_{\text{Sample }\lambda} - \varphi_{\lambda}) / (\tau_{\text{Reference }\lambda} - \varphi_{\lambda}) \text{ X } 100, \quad (2.1)$$

where, λ = Wavelength,

τ = Reflected and scattered radiation

φ = Stray light without any sample on the sample port

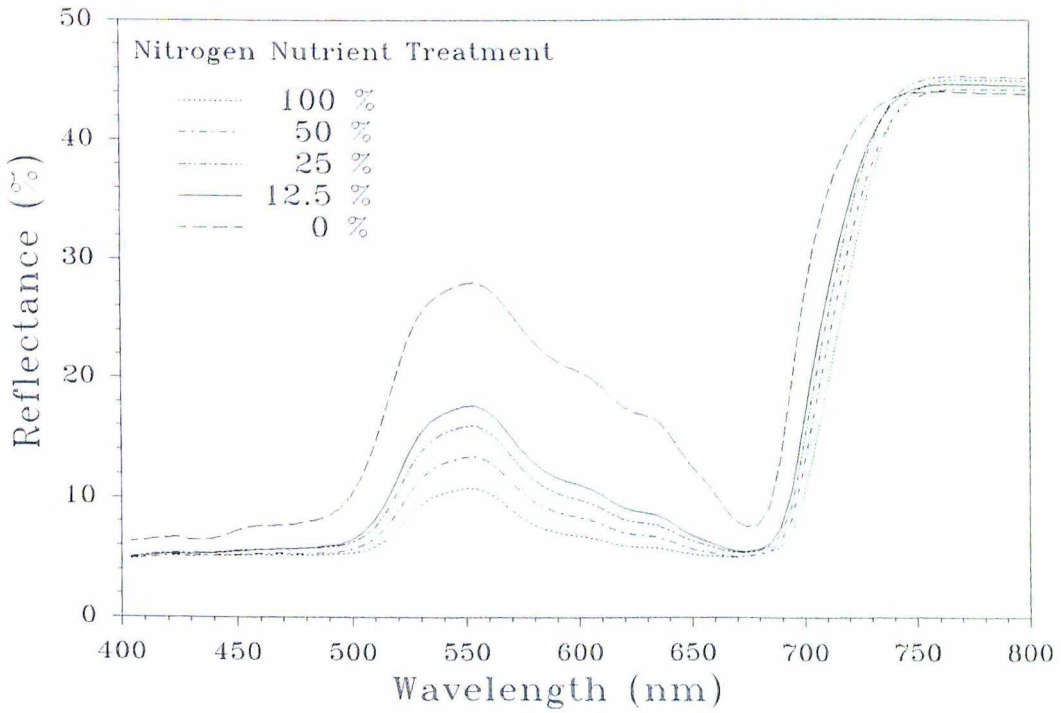

Figure 2.3 Mean reflectance spectra of nitrogen treated soybean leaves

Figure 2.3 presents the mean reflectance spectra for the five N-treated soybean leaves. The spectra illustrate the changes in reflectances caused by the varying N nutrient concentrations.

2.3.2 Pigment Concentrations

Chlorophyll a and b, and carotenoids were extracted from the same portion of the leaves that were used for the optical property measurements. Disks from the leaves were cut using a number 12 cork bore (2.5 cm^2). The pigments of the leaf samples were extracted in 5 ml of 100 % dimethyl sulfoxide (DMSO) for 24 hours in the dark (Hiscox and Israelstam, 1979). Absorbance of the assay solution was measured in a quartz cuvette with a light path length of 10 mm. The absorbance was determined using a Perkin-Elmer dual beam spectrophotometer which has 1 nm spectral resolution and a spectral range of 190 nm to 900 nm. The absorbance measurements were acquired from 300 nm to 750 nm at 1 nm interval at a speed of 120 nm/min. The spectrophotometer unit is equipped with a computer interface where the data can be transferred to a computer for further data processing.

The chlorophylls and carotenoid concentrations, were calculated from the spectra using equations described by Lichtenthaler et al. (1989) at 470 nm, 648 nm, and 664 nm, where

$$\text{Chlorophyll } a_c = 12.15A_{664\text{ nm}} - 2.79A_{648\text{ nm}},$$

$$\text{Chlorophyll } b_c = 21.50A_{648\text{ nm}} - 5.10A_{664\text{ nm}},$$

$$\text{Carotenoids}_c = (1000A_{470\text{ nm}} - 1.82\ \text{Chl}\ a_c - 85.02\ \text{Chl}\ b_c) / 198,$$

β carotene = $carotenoids_c$ / 3,

A = absorbance

c = pigment concentration (μg/mL of extract).

The concentration of the extracts are listed in table 2.1. It is observed that the pigment concentration decreases as the level of the nitrogen nutrient treatment decreases.

2.3.3 Soil Reflectance

Soil samples were obtained from National Soil Erosion Research Laboratory and BARC/USDA (Daughtry et al., 1993). Table 2.2 lists the locations and types of the soil samples used. The LI-1800 spectroradiometer used for the leaf level reflectance and a 150 watt xenon lamp were utilized for bidirectional soil reflectance measurements. The bidirectional radiance measurements of soils and barium sulfate surface as the reference were acquired with 15° field of view (FOV) at a nadir view angle and 20° illumination angle. Data processing procedures employed for the soil reflectance measurements were similar to the leaf measurements. Percent Reflectance value was calculated as the reflected radiance from the soil divided by the reflected radiance from the reference surface, multiplied by 100 (Eq. 2.2).

$$\text{Percent Soil Reflectance}_{\lambda} = (\tau_{\text{Soil }\lambda} / \tau_{\text{Reference }\lambda}) \text{ X } 100, \qquad (2.2)$$

where, λ = Wavelength,

τ = Reflected radiation

The reflectance spectra of the soil samples are shown in figure 2.4 where it illustrates broad ranges of soil reflectances.

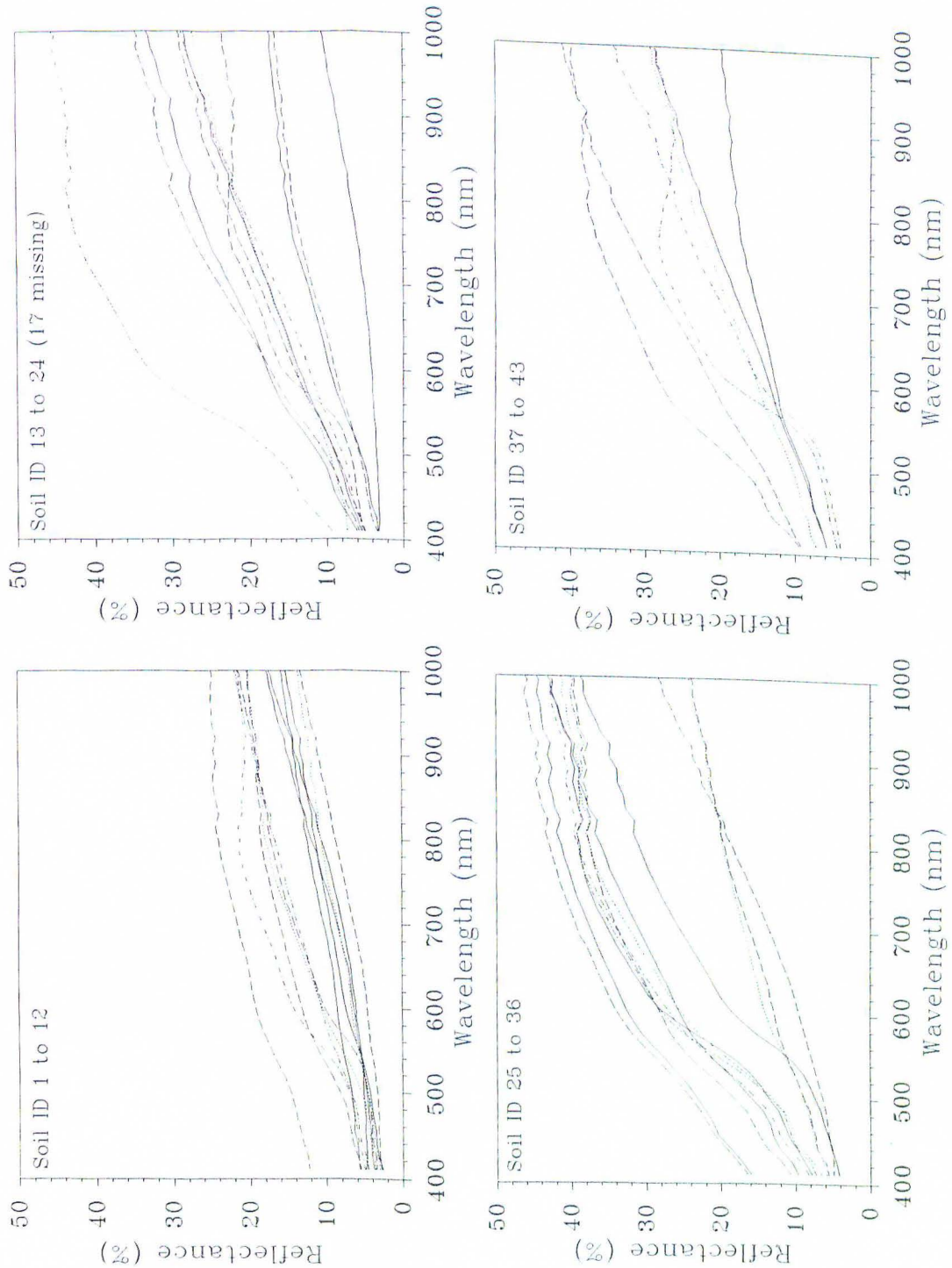

Figure 2.4 Reflectance spectra of soils

N Level	Rep Num	Chl *a*	Chl *b*	Chl *a+b*	Carotenoids	β-Cart
100%	1	14.206	5.042	19.248	3.678	1.226
100%	2	14.794	5.383	20.177	3.482	1.161
100%	3	18.123	9.108	27.231	4.816	1.606
100%	4	17.696	8.765	26.461	4.270	1.423
100%	5	19.056	11.335	30.391	5.224	1.741
100%	6	18.743	9.562	28.305	4.811	1.604
100%	7	18.434	9.526	27.960	4.570	1.523
100%	8	18.089	9.590	27.679	4.753	1.584
100%	9	14.684	5.457	20.142	2.874	0.958
100%	10	13.836	5.277	19.114	3.213	1.071
50%	1	15.201	6.019	21.220	3.993	1.331
50%	2	13.639	5.083	18.722	3.613	1.204
50%	3	15.790	6.347	22.137	3.725	1.242
50%	4	16.652	6.934	23.586	3.714	1.238
50%	5	13.440	4.584	18.024	3.504	1.168
50%	6	14.147	5.640	19.787	3.552	1.184
50%	7	12.431	4.888	17.319	3.253	1.084
50%	8	14.732	6.485	21.217	3.793	1.264
50%	9	12.277	4.753	17.030	3.102	1.034
50%	10	12.705	5.144	17.849	3.507	1.169
25%	1	9.553	3.292	12.845	2.539	0.846
25%	2	13.686	4.974	18.660	3.327	1.109
25%	3	10.563	3.785	14.347	2.663	0.888
25%	4	10.879	4.001	14.880	2.858	0.953
25%	5	11.324	4.039	15.363	2.902	0.967
25%	6	11.666	4.411	16.077	3.034	1.012
25%	7	15.146	5.981	21.127	3.952	1.317
25%	8	13.083	4.946	18.029	3.314	1.105
25%	9	12.308	4.716	17.023	3.013	1.004
25%	10	12.859	5.131	17.990	3.273	1.091
12.5%	1	12.199	4.529	16.728	3.014	1.005
12.5%	2	10.702	3.900	14.602	2.687	0.896
12.5%	3	9.338	3.396	12.733	2.299	0.766
12.5%	4	8.649	3.099	11.748	2.225	0.742
12.5%	5	11.047	4.023	15.069	3.001	1.000
12.5%	6	10.745	4.238	14.983	2.719	0.906
12.5%	7	9.623	3.639	13.262	2.565	0.855
12.5%	8	8.880	3.493	12.373	2.196	0.732
12.5%	9	9.938	3.786	13.724	2.489	0.830
12.5%	10	7.335	2.790	10.124	1.872	0.624
0%	1	2.842	1.123	3.965	0.724	0.242
0%	2	2.357	0.945	3.302	0.605	0.202
0%	3	3.099	1.246	4.345	0.844	0.281
0%	4	3.893	1.530	5.423	1.007	0.336
0%	5	2.754	1.111	3.865	0.741	0.247
0%	6	2.702	1.118	3.821	0.737	0.246
0%	7	4.351	1.744	6.095	1.171	0.391
0%	8	3.731	1.656	5.387	0.991	0.330
0%	9	3.154	1.410	4.565	1.051	0.350
0%	10	4.163	1.861	6.024	1.276	0.425

Table 2.1 DMSO extracted pigment concentration (μg/ml) for nitrogen nutrient treated soybean leaves.

SOIL SAMPLES

Location			Soil Type	Location			Soil Type
1	Albin	WO	Keith	23	Como	MS	Loring
2	McClusky	ND	Williams	24	Lincoln	NB	Sharpburg
3	Flintstone	MD	Opaquin	25	Columbia City	IN	Lewisburg
4	Ames	IA	Clarion	26	Ord	NE	Hersh
5	Castana	IA	Monona	27	McClusky	ND	Williams
6	Pullman	WA	Palouse	28	Waco	TX	Heiden Clay
7	Pullman	WA	Walla Walla	29	Wall	SD	Pierre Clay
8	Watkinsville	GA	Hiawassee	30	Scottsbluff	OK	Keith
9	Morris	MN	Sverdrup	31	Buffalo	OK	Woodward
10	Twin Falls	ID	Portneuf	32	Fresno	CA	Whitney
11	Morris	MN	Barnes	33	Salisbury	NC	Gaston
12	Los Banos	CA	Los Banos	34	Watkinsville	GA	Cecil
13	Waveland	IN	Miami	35	Hancock	MD	Frederick
14	Ellicott City	MD	Manor	36	Dayton	OH	Miamian
15	Tifton	GA	Bonifay	37	Como	MS	Grenada
16	Fresno	CA	Academy	38	*Beltsville	MD	Dark
18	Big Springs	TX	Amarillo	39	*Beltsville	MD	Red
19	Columbia	MO	Mexico	40	*Beltsville	MD	Light
20	Bainville	MT	Zahl	41	*Beltsville	MD	Codorus
21	Presque Isle	ME	Caribou	42	*Beltsville	MD	Sand
22	Tifton	GA	Tifton	43	*Beltsville	MD	Peat

Table 2.2 Soil locations and types used for reflectance measurements. Soils from National Soil Erosion Research Lab. Soil number 17 is missing and soils 38 to 43 were collected independently by Dr. Daughtry at BARC/USDA.

2.4 The SAIL Model Simulated Canopy Reflectance and f_{apar}

Computer source code (VAX: FORTRAN) for the SAIL model was made available by Mr. F. Hummerich of Hughes STX Inc., and the code was modified to a PC Qbasic version by the author. Soybean canopy reflectances at 10 nm spectral resolution at 550, 670, 700 nm, and 600-690 nm and 750-850 nm were simulated using the SAIL model. The mean soybean optical properties of 50% N treatment were used for the model input. Table 2.3 lists the optical properties and parameters used for the

Table 2. 3 Soybean leaf reflectance and transmittance plus other input parameters used for the SAIL model simulation of soybean canopy reflectance.

Waveband	% Refl.	% Trans.	SOLAR TIME	11:00
550 ± 5 nm	12.88	18.03	SOLAR DECLINATION ANGLE	23.50°
670 ± 5 nm	5.83	3.18	SOLAR ZENITH ANGLE	20.79°
700 ± 5 nm	14.80	20.23	LATITUDE	40.00°
RED (600-690 nm)	6.87	6.98	VIEW ZENITH ANGLE	0.00°
NIR (750-850 nm)	45.85	52.47	VIEW AZIMUTH ANGLE	0.00°

simulation. The reflectance and transmittance of the red and NIR band were the mean values calculated from the narrow band optical properties in the spectral range of 600 nm to 690 nm, and 750 nm to 850 nm, respectively. Reflectances of soils obtained from National Soil Erosion Research Laboratory were used to provide values of background materials in the simulation of canopy reflectance. 20 levels of LAI ranging from 0.1 to 4.5 (0.1 to 1.0 in 0.1 interval, 1.25, 1.5, 1.75, 2, 2.25, 2.5, 3, 3.5,

4, and 4.5), with 42 different soils as background were simulated giving a total of 840 canopy reflectance measurements. In conjunction with these reflectance spectra, the fraction of absorbed photosynthetically active radiation (f_{apar} = [A_{par} / Incident PAR]: Daughtry et al., 1992) were simulated.

Figure 2.5 illustrates the model input spectra and the simulated canopy reflectances at various LAIs ranging from 0.05 to 5.0. Note that the canopy reflectances increase in the NIR region and decrease in the VIS region as a function of the LAI.

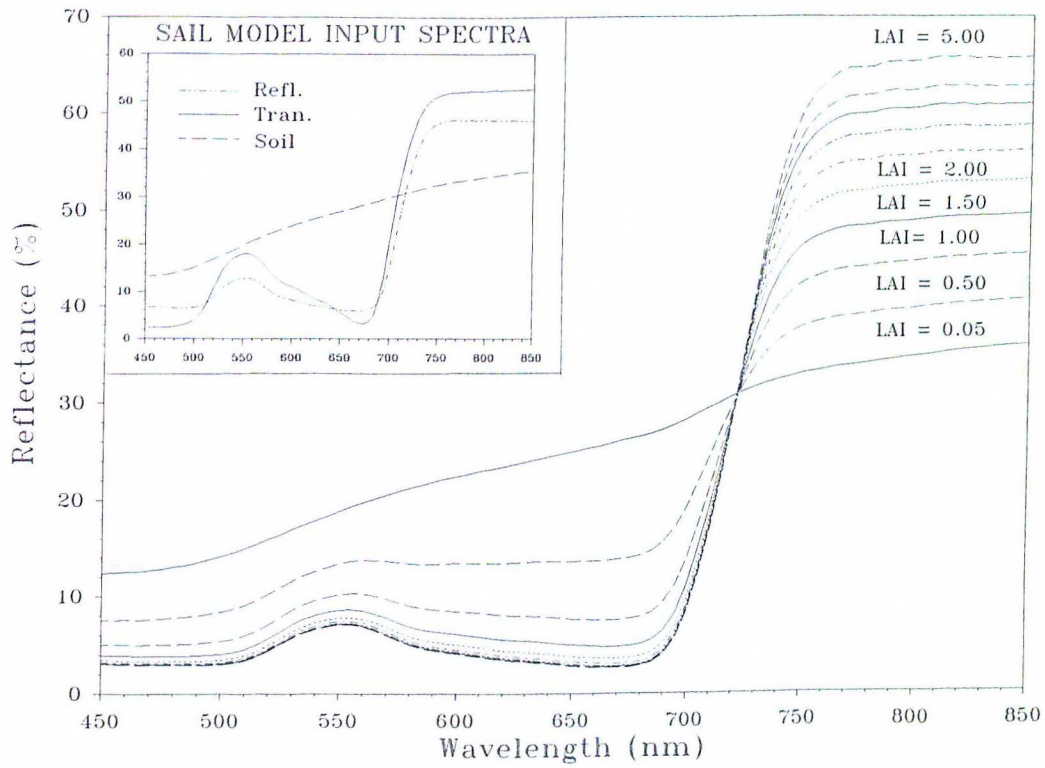

Figure 2.5 Soybean canopy reflectance simulated from the SAIL model. LAI ranges from 0.05 to 5.0.

CHAPTER 3. DEVELOPMENT OF CHLOROPHYLL ABSORPTION RATIO INDEX (CARI)

3.1 Introduction

The fundamental basis of this research in developing a narrow band method to estimate f_{apar} is based on the absorption characteristics of plant pigments which have direct effects on reflectance. The development of the narrow band method involved a similar approach to that of mineralogical analysis techniques. Studies have reported the successful use of absorption characteristics in the assessment of mineral features in reflectance (Green et al., 1985; Kruse et al., 1985; Clark et al., 1987).

Mineralogical analysis techniques exploit the absorption properties of minerals in the NIR reflectance spectra to characterize mineral contents. This technique defines a continuum by fitting a line between two high points in the reflectance spectrum. The original reflectance is divided by the continuum to normalize the absorption band to a common reference value of one. Thus, the area of absorption is less than one but greater than zero. The continuum-removed spectrum which produces the depth, width, asymmetry, and wavelength position of the continuum-removed spectrum are related to mineral absorption characteristics.

Absorbance of Photosynthetic Pigments - Solar radiation in the PAR region is absorbed by plant pigments. The pigments making the greatest contribution to light absorption are chlorophyll a, chlorophyll b, and carotenoids (Fig. 3.1). Both chlorophylls a and

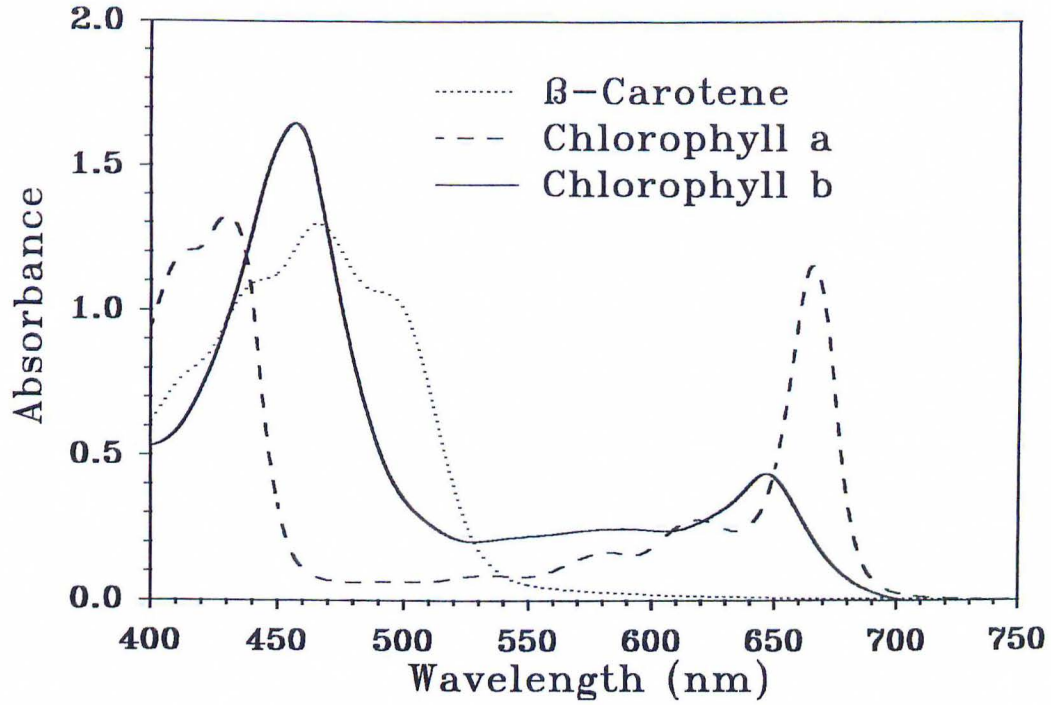

Figure 3.1 Absorbance of pure plant pigments (Absorbance = log (I_0/I), I_0 = incident, I = transmitted light). Redrawn from Chappelle et al., (1992).

b have absorption maxima in the 640 - 690 nm region and in the 440 - 470 nm region. Also, β-carotene has broad absorption peak in the 470 nm region and minimum absorption beyond 530 nm. Chlorophylls and β-carotene have minimal absorption at 550 nm region. Beyond 700 nm, these pigments do not absorb any radiation.

3.2 Significance of 550 and 700 nm bands in Leaf Level Reflectance

Many of the reflectance bands of the soybean leaf reflectance spectra were strongly correlated with each other (Table 3.1), especially in the PAR region. It

appears that the 550 nm and 700 nm bands have the highest correlation (r^2 = 0.992). This relationship is apparent in the absorption of the pure pigments (Fig. 3.1) in which

Table 3.1 Correlations (r^2) between soybean leaf reflectance (n = 50) bands. Reflectance measurements were acquired using LI-COR 1800 spectroradiometer and integrating sphere.

Wave(nm)	550	670	690	700	710	750	800
550	1.000	0.786	0.930	0.992	0.981	0.000	0.062
670	0.786	1.000	0.914	0.802	0.710	0.005	0.083
690	0.930	0.914	1.000	0.955	0.871	0.001	0.075
700	0.992	0.802	0.955	1.000	0.973	0.000	0.059
710	0.981	0.710	0.871	0.973	1.000	0.008	0.034
750	0.000	0.005	0.001	0.000	0.008	1.000	0.903
800	0.062	0.083	0.075	0.059	0.034	0.903	1.000

the 550 nm and 700 nm bands correspond to the minimum absorption of the photosynthetic pigments. The significance of this relationship is such that in leaf level reflectance, a ratio of the 550 nm and 700 nm bands is nearly constant regardless of the differences in pigment concentrations in the leaves. When the 550 nm bands are plotted against the 700 nm reflectance bands of the soybean leaves, the strength of this relationship is well illustrated (figure 3.2). It is observed that beyond 700 nm where absorption due to the pigments is minimal, the correlation with the 550 nm band drops. This is possibly due to the dominance of the effect of leaf structure on vegetative reflectance beyond 700 nm.

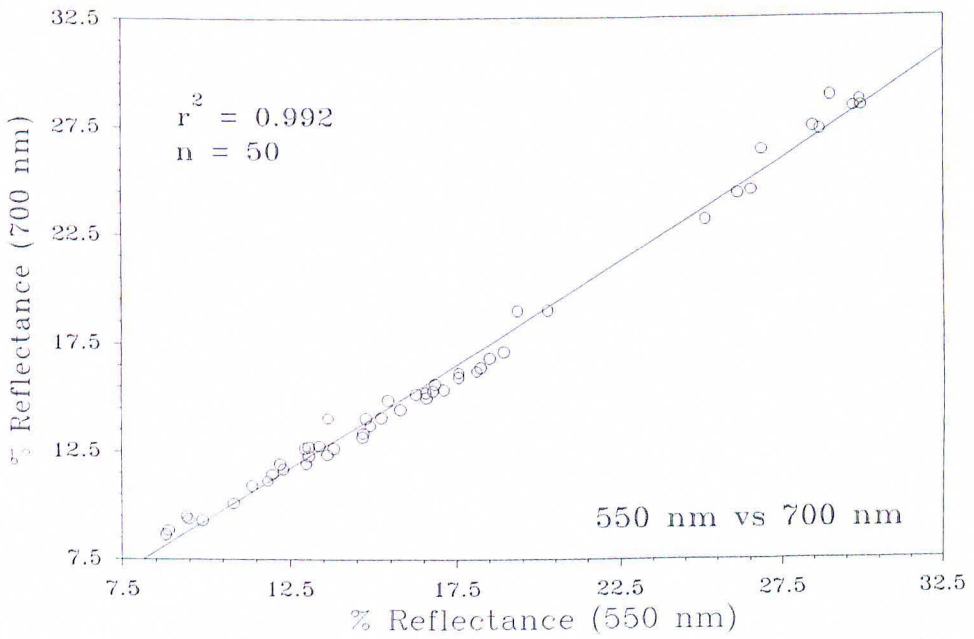

Figure 3.2 Scatter plot of soybean leaf reflectance (550 nm versus 700 nm)

The 700 nm band is located in the Red-NIR region (also known as "Red Edge"). It is a boundary between the regions where reflectance is dominated by the absorption characteristic of chlorophyll a and the beginning portion of the NIR reflectance which is due to the structural characteristics of vegetation. Thus, the transition from the dominant effect of the pigment absorption to NIR vegetative characteristics (i.e., scattering) occurs at this wavelength.

3.2.1 Definition of the Chlorophyll Absorption in Reflectance (CAR)

Utilizing the properties of the 550 nm and 700 nm bands in conjunction with the 670 nm chlorophyll a absorption maximum band led to the definition of the

chlorophyll absorption in reflectance (CAR). The line (a) in Fig. 3.3 (II) which was drawn from the 700 nm to 550 nm band is used as the base line to measure the depth of the chlorophyll absorption. The slopes of this 550 nm - 700 nm lines are a constant for the 50 soybean leaf level reflectance spectra. The distance (b) in Fig. 3.3 (II) from the 670 nm band perpendicular to the 550-700 nm line (absorption minima) is defined as CAR. Thus, CAR is the shortest distance from the 670 nm band to the 550 nm-700 nm line.

The calculation of the CAR utilizes an orthogonal projection on a 2-dimensional x-y plane using wavelength as the x coordinate and the percent reflectance as the y coordinate. By definition (Strang, 1980), the orthogonal projection p from a point to a vector spanned from the origin is given by in matrix form,

$$p = \frac{a^T b}{a^T a} \circ a, \qquad where\ a^T = (x_{700nm-550nm}\ y_{700nm-550nm}),\ a = \begin{pmatrix} x_{700nm-550nm} \\ y_{700nm-550nm} \end{pmatrix},\ b = \begin{pmatrix} x_{670nm-550nm} \\ y_{670nm-550nm} \end{pmatrix}.$$

Note that the wavelength and the reflectance coordinates are linearly transformed so that x_{550nm} and y_{550nm} become the origin of the x-y plane. Thus, the 550 nm-700 nm line is the vector spanned from the origin. The distance (CAR) of the projection from the point (670 nm) to the p is quantified as

$$CAR^2 = \left\| b - \frac{a^T b}{a^T a} \circ a \right\|^2 = \frac{(b^T b) \circ (a^T a) - (a^T b)^2}{(a^T a)} \quad then, \qquad CAR = \sqrt{\frac{(b^T b) \circ (a^T a) - (a^T b)}{(a^T a)}}$$

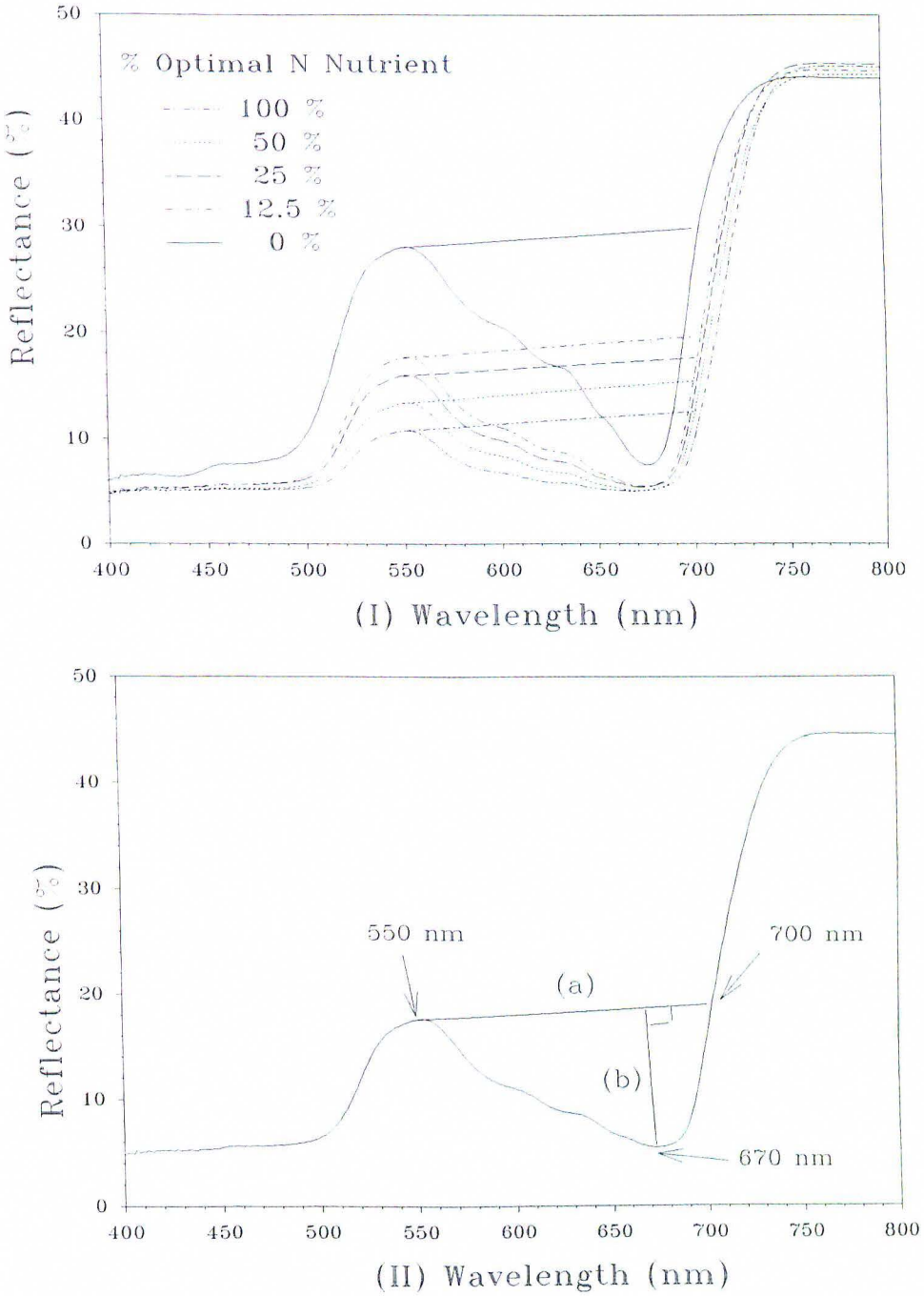

Figure 3.3 (I). Mean (n=10) reflectance spectra of nitrogen treated soybean leaves. (II). (a) is a chlorophyll absorption minima line, (b) is defined as CAR

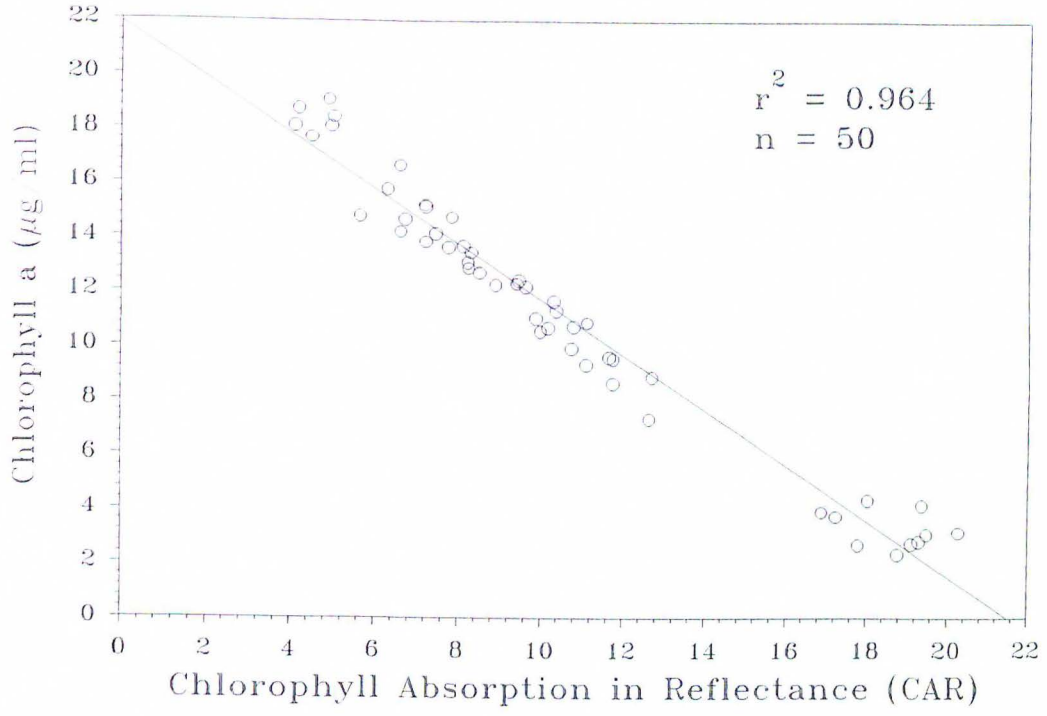

Figure 3.4 CAR of 50 soybean leaf reflectance vs chlorophyll a concentration of the same leaves

CAR calculated on the reflectance spectra of 50 soybean leaves plotted against the chlorophyll *a* concentrations are presented in figure 3.4. There is a strong inverse-linear relationship with a regression r^2 of 0.964 demonstrating the values of CAR as an accurate measurement of leaf level chlorophyll absorption.

3.3 Characteristics of Soil and Leaf Litter Reflectance

High spectral resolution reflectance spectra from 500 nm to 800 nm of nonphotosynthetic materials are shown in figure 3.5. Unlike the reflectance of spectra of green vegetation, absorption due to photosynthetic pigments at 670 nm was not

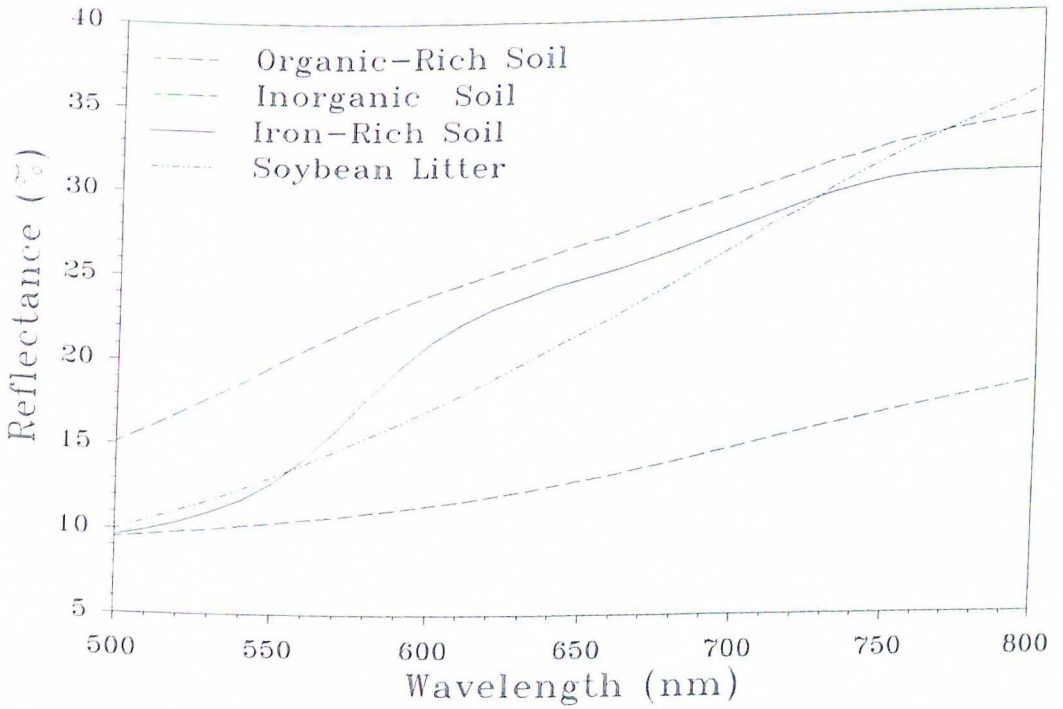

Figure 3.5 Reflectance spectra of nonphotosynthetic materials. Spectra acquired with LI-1800 integrating sphere radiometer.

observed in any of the spectra. Stoner et al. (1981) characterized and established general genetic, physical, and chemical relationships affecting each spectral curve characterization. The reflectance spectrum of the iron-rich soil has a rising slope at around 550 nm and a falling slope at around 750 nm due to the iron content of the soil. The inorganic soils and organic-rich soils exhibited monotonic increases in reflectance with wavelength. The reflectance spectrum of leaf litter displayed characteristics similar to the organic-affected and minimally-altered soils.

In the soil and litter reflectance spectra, the slopes of the lines drawn from 550 to 700 nm changed as functions of the reflectance characteristics of the materials where

in the case of green leaves the slope was constant. The ratios of reflectance at 700 nm and reflectance at 550 nm for the organic-rich soil, iron-rich soil, inorganic soil, and soybean litter are 1.44, 1.22, 1.43, and 1.2, respectively. Furthermore, the 670 nm band, in most of the reflectance spectra of nonphotosynthetic materials, is located close to or on the line spanned from 550 to 700 nm bands. Thus, the CAR of soils and leaf litter were near zero (CAR <= 0.5).

In summary, CAR is a spectral greenness index that is a good measurement of the pigment absorption in leaves. In the case of nonphotosynthetic materials, CAR is negligible. The key issue is whether the CAR concept is applicable to canopy reflectance which is a mixture of both green and nonphotosynthetic components.

3.4 Characteristics of CAR in Canopy Reflectance

Reflectance spectra of a soybean canopy, with an LAI of 1.0, were simulated using the SAIL model with the organic-rich, iron-rich, and inorganic soil, as background materials. Since the LAI for the canopy is 1.0, the simulated spectra contain identical green biomass and the only differences among the spectra are the effects of reflectance characteristics of the soils. Figure 3.6 illustrates the resulting spectral variabilities in the canopy reflectance due to the different background reflectances, and that the slopes of reflectance at 550 nm to 700 nm lines of CAR vary as a result of the effects of the background soil reflectances. The variations in canopy reflectance are recognized by differences between the reflectance at 700 nm to 550 nm band ratios which are 1.35, 1.44, and 1.70 for the organic-rich, inorganic, and iron-rich

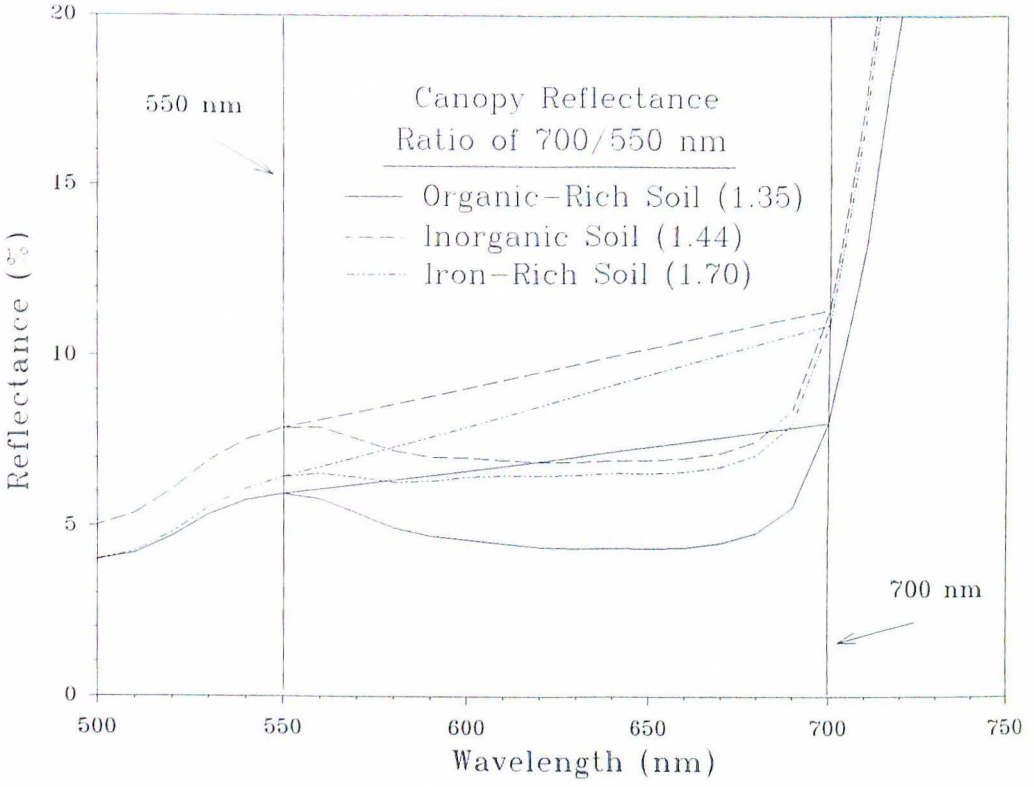

Figure 3.6 The SAIL model simulated soybean canopy reflectances. 700/550 nm ratio differences illustrate the effects of background materials.

soil, respectively. Also, the variations in reflectance values at 670 nm were noticed and were dependent upon the background reflectance.

Plots of the soybean canopy CAR and f_{apar} values, were both obtained from the SAIL model simulation using the same background materials as above (Fig. 3.7). This figure reveals variations in the relationship between the CAR values and f_{apar}. The variability of CAR in relation to f_{apar} represents the contribution of the variations in soil

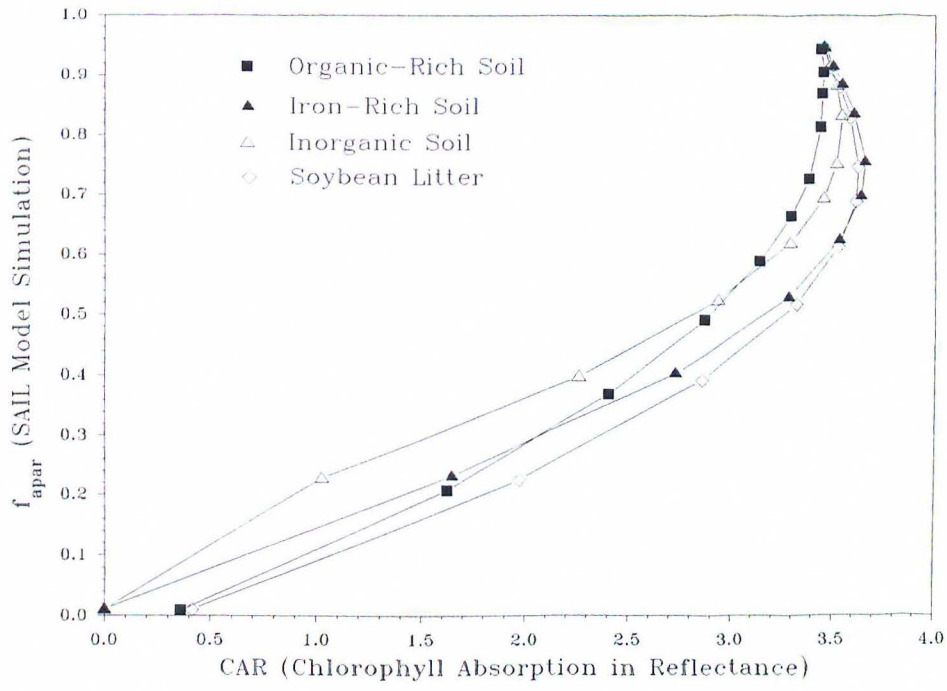

Figure 3.7 Relationship between the CAR and f_{apar}. The legends represent the types of background materials used in the SAIL model.

background reflectances. However, as the canopy becomes enclosed (LAI >= 3.0) the CAR values converges to a single value. This is an indication that the effects of soil reflectance in CAR is less when canopy is fully enclosed, and is a function of canopy cover in the intermediate canopy closure. Also, the hyperbolic (concave down) relationship between CAR and f_{apar} indicates that CAR values under-estimate f_{apar} in the incomplete canopy closure.

In summary, the changes in the reflectance at 550 nm to 700 nm slope and reflectance at 670 nm were noticed due to the variations in background reflectances.

Variations in CAR were the result of two factors; 1) the reflectance characteristics of various nonphotosynthetic background materials; and 2) canopy cover (i.e., fraction of vegetation to the background material). These factors appear to interact with each other in affecting overall canopy reflectance, and as a result, the CAR under-estimates f_{apar}.

3.5 Development of the Chlorophyll Absorption Ratio Index (CARI)

Although CAR appears to be a suitable greenness index for estimating absorption from leaf level reflectance spectra, it was found to under estimate f_{apar} at the canopy level. Canopy level CAR is a function of absorption due to green vegetation and reflectance characteristics of background materials. The canopy level CAR was modified to compensate for the effects of background reflectance leading to under-estimation of f_{apar}.

A multiplication of the reflectance band ratio of 700 nm and 670 nm with CAR, was defined as the chlorophyll absorption ratio index (CARI). It is defined as:

$$CARI = CAR_{canopy} \cdot (\rho_{(700)} / \rho_{(670)}), \text{ where } \rho = \text{percent reflectance.}$$

The ratio of the 700 nm and 670 nm bands counteracts the effects of background reflectance in CAR. These bands were chosen since, at 670 nm, chlorophyll a in vegetation has an absorption maximum which minimizes the background reflectance. The 700 nm band where chlorophyll a absorption becomes a minimum is also the band where the background reflectance becomes relatively significant. These bands are located closely such that changes in reflectance for background soil are small (i.e.,

$\rho(700) - \rho(670) <= 1.5$) compared to reflectance differences due to vegetation (i.e.,$\rho(700) - \rho(670) >= 5$).

3.5.1 Ratio of 700 nm and 670 nm Bands

The role of the $\rho_{(700)} / \rho_{(670)}$ ratio in the vegetation-background canopy system can be explained as follows: Reflectance of a vegetation canopy is expressed as a linear sum of green biomass and background components (linear additive model of two components) and is written as

$$\Phi(g,b) = \rho_{c(\lambda)} = \gamma \cdot \rho_{g(\lambda)} + (1-\gamma) \cdot \rho_{b(\lambda)}, \quad (3.1)$$

where γ is the fraction of the green biomass that occupies a scene (field of view of a sensor). Thus, $(1-\gamma)$ is the fraction of the background material. The letters c, g, and b in Eq. 3.1 stand for canopy, green biomass, and background. A vegetation canopy reflectance at 700 nm is expressed as

$$\rho_{c(700)} = \gamma \cdot \rho_{g(700)} + (1-\gamma) \cdot \rho_{b(700)}. \quad (3.2)$$

Then, the green biomass component in Eq. 3.2 can be rewritten as

$$\rho_{g(700)} = \rho_{g(670)} + \Delta\rho_g \approx \rho_{g(670)} + \Delta\alpha, \quad (3.3)$$

where $\Delta\rho_g$ is a difference in reflectance between 670 nm and 700 nm that are mainly due to chlorophyll a absorption maximum and minimum. Thus, the differences in reflectance at these wavelength were substituted with the contribution of chlorophyll a absorption ($\Delta\alpha$). Likewise, the background component in Eq. 3.2 is

$$\rho_{b(700)} = \rho_{b(670)} + \Delta\rho_b. \quad (3.4)$$

Since canopy backgrounds such as soils reflectance do not have distinctive absorption

features between 670 nm and 700 nm, $\Delta\rho_b$ is a change of background reflectance between 670 nm and 700 nm. $\rho_{g(700)}$ and $\rho_{b(700)}$ in Eq. 3.2 are substituted with the right sides of Eq. 3.3 and Eq. 3.4, respectively. Thus,

$$\begin{aligned}\rho_{c(700)} &= \gamma\cdot(\rho_{g(670)} + \Delta\alpha) + (1-\gamma)\cdot(\rho_{b(670)} + \Delta\rho_b) \\ &= \gamma\cdot\rho_{g(670)} + (1-\gamma)\cdot\rho_{b(670)} + \gamma\cdot\Delta\alpha + (1-\gamma)\cdot\Delta\rho_b \\ &= \rho_{c(670)} + \gamma\cdot\Delta\alpha + (1-\gamma)\cdot\Delta\rho_b,\end{aligned} \tag{3.5}$$

and since $\rho_{c(670)}$ can be rewritten as $\gamma\cdot\rho_{c(670)} + (1-\gamma)\cdot\rho_{c(670)}$ Eq. 3.5 becomes

$$\begin{aligned}\rho_{c(700)} &= \gamma\cdot\rho_{c(670)} + (1-\gamma)\cdot\rho_{c(670)} + \gamma\cdot\Delta\alpha + (1-\gamma)\cdot\Delta\rho_b \\ &= \gamma\cdot(\rho_{c(670)} + \Delta\alpha) + (1-\gamma)\cdot(\rho_{c(670)} + \Delta\rho_b)\end{aligned} \tag{3.6}$$

The numerator in the ratio $\rho_{c(700)} / \rho_{c(670)}$ is substituted with Eq. 3.6, and therefore,

$$\begin{aligned}\rho_{c(700)} / \rho_{c(670)} &= [\gamma\cdot(\rho_{c(670)} + \Delta\alpha) + (1-\gamma)\cdot(\rho_{c(670)} + \Delta\rho_b)] / \rho_{c(670)} \\ &= \gamma\cdot[(\rho_{c(670)} + \Delta\alpha) / \rho_{c(670)}] + (1-\gamma)\cdot[(\rho_{c(670)} + \Delta\rho_b) / \rho_{c(670)}]\end{aligned} \tag{3.7}$$

The ratio becomes a sum of the fraction changes in green biomass (absorption) component and that of the background component. Finally, the multiplication of Eq. 3.7 to CAR_{canopy}, CARI becomes,

$$\begin{aligned}CARI &= CAR_{canopy}\cdot\{\gamma\cdot[(\rho_{c(670)} + \Delta\alpha) / \rho_{c(670)}] + (1-\gamma)\cdot[(\rho_{c(670)} + \Delta\rho_b) / \rho_{c(670)}]\} \\ &= \gamma\cdot\{CAR_{canopy}\cdot[(\rho_{c(670)} + \Delta\alpha) / \rho_{c(670)}]\} + \\ &\quad (1-\gamma)\cdot\{CAR_{canopy}\cdot[(\rho_{c(670)} + \Delta\rho_b) / \rho_{c(670)}]\}.\end{aligned}$$

CARI is thus the sum of CAR_{canopy} proportionally weighed according to the fraction changes in reflectance due to vegetation (i.e., absorption of chlorophyll a) and

background components. In full canopy closure ($\gamma = 1$), the term $(1-\gamma) \cdot\{CAR_{canopy} \cdot [(\rho_{c(670)} + \Delta\rho_b) / \rho_{c(670)}]\}$ becomes zero. Thus, CARI is a function of CAR_{canopy} weighed by the vegetation component. In contrast, when $\gamma = 0$ (bare background soil), CARI is near zero or a very small quantity since CAR_{canopy} is near zero. In the case of partial canopy closure, under estimated f_{apar} in CAR_{canopy} due to the background effects are compensated by the addition of CAR_{canopy} multiplied by background factor, $(1-\gamma) \cdot[(\rho_{c(670)} + \Delta\rho_b) / \rho_{c(670)}]$.

CHAPTER 4. ASSESSMENT OF CARI

Soybean canopy reflectance at 10 nm spectral resolution at 550, 670, 700 nm, and 600-690 nm and 750-850 nm bands were simulated using the SAIL model. A total of 840 canopy reflectances, 20 levels of LAI ranging from 0.1 to 4.5 (0.1 to 1.0 in 0.1 interval, 1.25, 1.5, 1.75, 2, 2.25, 2.5, 3, 3.5, 4, and 4.5), with 42 different soils as background were simulated. Also, f_{apar} for these LAIs were simulated using a mean reflectance and transmittance in the wavelength region of 500 - 670 nm.

Figure 4.1 is a presentation of vegetation indices plotted against f_{apar}. These

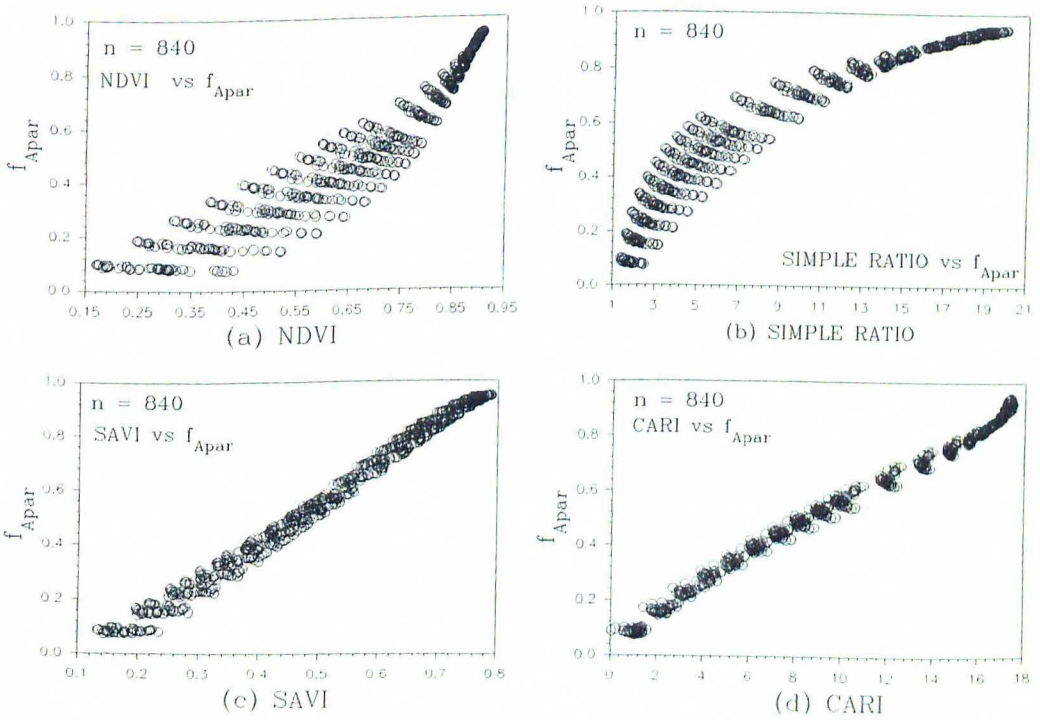

Figure 4.1 Relationship between Vegetation indices and fraction of absorbed photosynthetically active radiation (f_{apar})

VIs were calculated using the results from the SAIL model simulation. The NDVI was calculated using (NIR - RED) / (NIR + RED). For the calculation of the SAVI (Huete, 1988 and 1989), a soil isoline factor of 0.5 resulted in the smallest variation for canopies with LAI less than or equal to 2. Thus, SAVI was calculated as [(NIR - RED) / (NIR + RED + 0.5)] X (1.5). The ratio of 750-850 nm and 600-690 nm were used for the SR. Before full canopy closure, the NDVI (figure 4.1(a)) and SR (figure 4.1(b)) are highly variable in the assessment of f_{apar} due to the variations in the soil background reflectance. The effects of soil backgrounds were significantly reduced by the SAVI (figure 4.1(c)) and CARI (figure 4.1(d)).

In order to test sensitivities of these VIs to the varied background soils, an "inversion" technique was used. Inversion of canopy reflectance models has been used to estimate vegetative variables (Goel et al., 1984). The SAIL model simulates canopy reflectance and f_{apar} at a given LAI. By inverting the SAIL model, LAIs were calculated using mean f_{apar} values and VIs obtained from the above simulation at LAI of 0.1, 0.5, 1.0, 1.5, 2.0, and 3.0 (figure 4.2). The plots of standard deviations (figure 4.2(a)) and coefficients of variation [(standard deviation / mean) X 100]: figure 4.2(b) illustrates the degree of sensitivities in these VIs to various background soils. The CARI displays the most insensitive response to the spectral variations of background soils at the LAI range less than 2.0 (i.e., before full canopy closure). The NDVI and SR are sensitive to the soil backgrounds at lower LAI ranges and become insensitive to the soil backgrounds at higher LAIs.

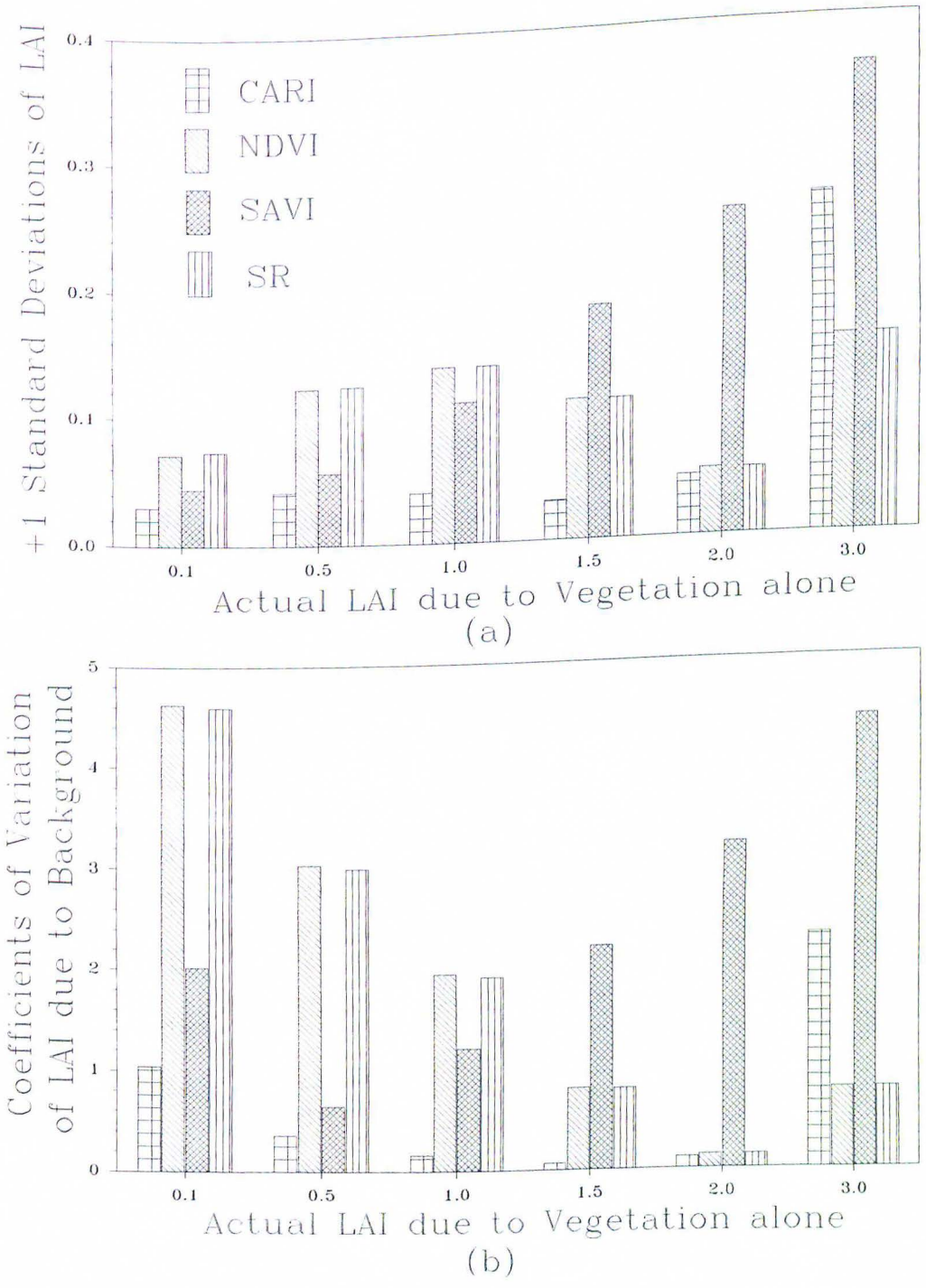

Figure 4.2 Sensitivities of vegetation indices to spectral variabilities of background soils.

To compare variability of these vegetation indices at lower LAIs, canopy reflectances were simulated at LAI ranging from 0.05 to 2.0 in 0.05 intervals, and the vegetation indices were calculated. The parameters used for this simulation were the same as the previous simulation. The statistical procedure Student-Newman-Kuels mean test was conducted to these vegetation indices. Table 4.1 is a presentation of the test results, where different letters indicate that the LAI values can be separated at a significance level of 99% (α=0.01, n=39). The result indicates that the CARI performs better than other broad band indices in differentiating the means at LAI differences of 0.05. Figure 4.3 is an illustration of the means and standard deviations of these

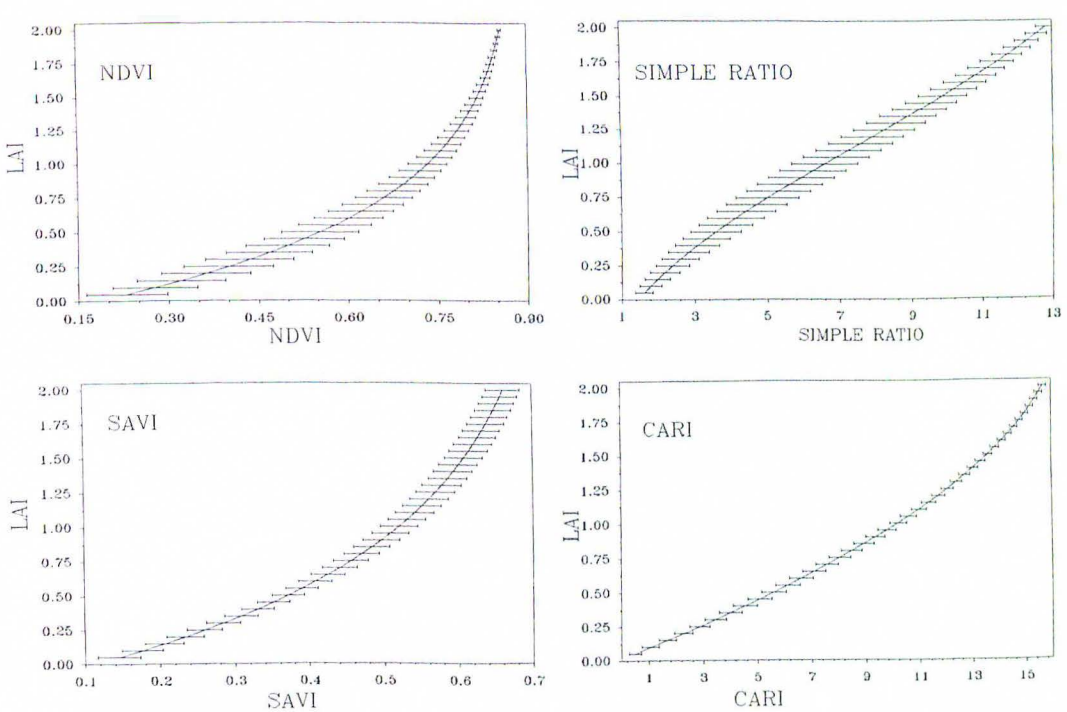

Figure 4.3 Relationship between LAI and Means and standard deviations of vegetation indices

vegetation indices plotted against LAI. This figure summarizes the effect of CARI in reducing effects of nonphotosynthetic materials in the assessment of vegetation canopy f_{apar} and it does this more effectively than broad band vegetation indices.

Table 4.1 Student-Newman-Kuels test for variables at a significance level of 99% ($\alpha = 0.01$, n = 39), where different letters indicate that LAI values can be separated. The table illustrates that the CARI performs better than other broad band indices in separating the means at LAI differences of 0.05.

LAI	SNK (CARI)	SNK (NDVI)	SNK (SAVI)	SNK (SR)
2.00	A	A	A	A
1.95	B A	A	B A	B A
1.90	B	B A	B A C	B C
1.85	C	B A	B D A C	D C
1.80	D	B A C	B D E C	D E
1.75	E	B A C	D E C	F E
1.70	F	B D A C	F D E	F G
1.65	G	B D A C	F E G	H G
1.60	H	E B D A C	F H G	H I
1.55	I	E B D A C F	I H G	J I
1.50	J	E B D C F	I H J	J K
1.45	K	E D G C F	I K J	L K
1.40	L	E H D G F	K J	L M
1.35	M	E H G F	L K	N M
1.30	N	H G I F	L M	N O
1.25	O	H J G I	N M	P O
1.20	P	H J K I	N O	P Q
1.15	Q	J K I	P O	R Q
1.10	R	L J K	P Q	R S
1.05	S	L K M	R Q	T S
1.00	T	L N M	R S	T U
0.95	U	N M	T S	V U
0.90	V	O N	T U	V W
0.85	W	O P	V U	X W
0.80	X	Q P	V	X Y
0.75	Y	Q R	W	Z Y
0.70	Z	S R	X	Z A'
0.65	A'	S T	Y	B'A'
0.60	B'	U T	Z	B'C'
0.55	C'	U V	A'	D'C'
0.50	D'	V	B'	D'E'
0.45	E'	W	C'	F'E'
0.40	F'	X	D'	F'G'
0.35	G'	Y	E'	H'G'
0.30	H'	Z	F'	H'I'
0.25	I'	A'	G'	J'I'
0.20	J'	B'	H'	J'I' K'
0.15	K'	C'	I'	J'L' K'
0.10	L'	D'	J'	L' K'
0.05	M'	E'	K'	L'

CHAPTER 5. CONCLUSIONS AND RECOMMENDATIONS

5.1 Conclusions

These investigations demonstrate the potential utility of narrow reflectance bands for assessing biophysical properties of vegetation canopy. The variability of broad band techniques due to background reflectance characteristics are significantly reduced by CARI.

It should be stressed that these conclusions are based solely upon the results obtained with simulated canopy reflectances and that the SAIL model does not consider all the natural phenomena in a vegetation canopy such as spectral variability due to woody biomass. Field experiments are planned to evaluate, and further enhance the utility of CARI.

5.2 Recommendations

The EOS (Earth observing system) sensors will be deployed in late 90s to observe many of the key variables and processes of the global scale cycles of energy, water, and biogeochemicals. One of the EOS platform will contain a high spectral resolution radiometers, MODIS-T and MODIS-N with a spectral resolution of 10 nm (narrow band) in the PAR region. This sensors will provide long term measurements of biophysical processes to improve understanding of the dynamics and processes occurring on the Earth surface. Some of the specific roles of the instrument are to provide measurements of net prime productivity, leaf area index, land cover type,

vegetation indices corrected for atmosphere, and A_{par}.

It would be of considerable value to EOS to be able to evaluate high resolution spectroscopy data with improved capability in the assessment of the biophysical processes of the planet. This research was designed to investigate the use of high spectral resolution sensing versus broad band techniques in the estimates of f_{apar}. The broad band vegetation indices currently used in estimating f_{apar} are sensitive to nonphotosynthetic materials such as soil and leaf litters. This research demonstrated effective use of high resolution spectroscopy in minimizing errors in estimates of f_{apar} due to interference of the nonphotosynthetic background in the vegetation canopy reflectance.

Remote sensing applications of high resolution spectroscopy is relatively new and interpretive algorithms for its use lag behind the technological advancement in instrumentation. Narrow band sensors on the airborne platforms are being flown, and narrow band satellite sensors will be deployed in the near future. The comparisons between the narrow band VIs (NDVI, SAVI, SR) and the broad band VIs showed functional equivalence. It is the responsibilities of remote sensing researchers, especially those who are interested in high spectral resolution spectroscopy, to develop quantitative analysis methods utilizing narrow band reflectance.

In closing, the cost involved in association with number of bands in high spectral resolution sensor design is a major concern to researchers and funding agencies. This research utilized three narrow bands to successfully improve accuracy in remote assessment of f_{apar}. More research is recommended for isolating vital narrow

bands for remote sensing applications. This will reduce the number of bands and, thus, should provide more cost-effective systems.

REFERENCES

Asrar, G., Fuchs, M., Kanemasu, E. T., and Hatfield, J. L. (1984), Estimating absorbed photosynthetic radiation and leaf area index from spectral reflectance measurements in wheat, *Agron. J.*, 76:300-306

Asrar, G., Kanemasu, E.T., Jackson, R.D., and P|inter, P.J. (1985), Estimation of total above ground phytomass production using remotely sensed data, *Remote Sens. Environ.*, 17:211-220

Asrar, G., Myneni, R. B., and Kanemasu, E. T. (1989), Estimation of plant-canopy attributes from spectral reflectance measurements, in Theory and Applications of Optical Remote Sensing (G. Asrar, Ed), Wiley, New York, pp. 252-296

Badhwar, G.D. (1985), Comparative Study of Suits and SAIL Canopy Reflectance Models, *Remote Sens. of Environ.*, 16:125-141

Baret, F., Guyot, G., and Major, D. (1989), TSAVI: a vegetation index which minimizes soil brightness effects on LAI and APAR estimation, in 12th Canadian Symp. on Remote Sensing and IGARSS'90, Vancouver, Canada, 10-14 July, 1989, 4. pp

Baret, F., and Guyot, G. (1991), Potentials and limits of vegetation indices for LAI and APAR assessment, *Remote Sens. of Environ.*, 35:161-174

Chappelle, E.W., Kim, M.S., and McMurtrey, J. (1992), Ratio Analysis of Reflectance Spectra (RARS): An Algorithm for the Remote Estimation of the Concentrations of Chlorophyll A, Chlorophyll B, and Carotenoids, *Remote Sens. Environ.*, 39:239-247

Chorowicz, J., Lavreau, J., Tamain, G. (1990), The evaluation of satellite imagery and field spectro-radiometer data for the study of the lithology and the aciont and reactivation tectonics in the vincinity of the East African Rift, *J. Photogrammetry and Remote Sens.*, 10

Choudhury, B.J. (1987), Relationships between vegetation indices, radiation absorption and net photosynthesis evaluated by sensitivity analysis, *Remote Sens. Environ.*, 22:209-233

Collins, W., Chang, S.H., Raines, G., Canney, F., and Ashley, R., (1983), Airborne Biogeochemical Mapping of Hidden Mineral Deposits, *Econ.. Geol.*, 78, 737-749

Collins,W. (1978) Remote Sensing of Crop Type and Maturity, *Photogramm. Eng. Remote Sensing*, 44, 43-55

Colwell, J.E. (1974), Vegetation canopy reflectance, *Remote Sens. Environ.*, 3:175-183

Daughtry, C.S.T., Ranson, K.J., Biehl, L.L. (1989), A New Technique to Measure the Spectral Properties of Conifer Needles, *Remote Sens. of Environ.*, 27:81-91

Daughtry, C.S.T., Gallo, K.P., Goward, S.N. and Prince, S.D. (1992), Spectral Estimates of Absorbed Radiation and Phytomass Production in Corn and Soybean Canopies, *Remote Sens. Environ.*, 39:141-152

Daughtry, C.S.T, McMurtrey, J.E., Chappelle, E.W., Dulaney, W.P., Irons, J.R., and Satterwhite, M.B. (1993), Potential for discriminating crop residues from soil by reflectance and fluorescence technique, Int. Geoscience Remote Sensing Symp. Tokyo, Japan. IGARSS'93 Digest 3:1325-1328

Demetriades-Shah, T.H., Steven, M.D., Clark, J.A. (1990), High Resolution Derivative Spectra in Remote Sensing, *Remote Sens. of Environ.*, 33:55-64

Dusek, D.A., R. D. Jackson, J. T. Musick, (1985), Winter Wheat Vegetation Indices Calculated from Combinations of Seven Spectral Bands, *Remote Sens. Environ.*, 18:255-267

Gallo, K.P., Daughtry, C.S.T., (1987), Differences in Vegetation Indices for Simulated Landsat-5 MSS and TM, NOAA-9 AVHRR, and SPOT-1 Sensor System, *Remote Sen. of Environ.*, 23:439-452

Gates, D.H., Keegan, H.J., Schleter, J.C., and Weidner, Spectral Properties of Plants, *Appl. Optics.*, 4, 273-278, 1965.

Gautheir, R.P. and Neville, R.A., (1985), Narrow Band Multispectral Imagery of the Vegetation Red Reflectance Edge for Use in Geobotanical Remote Sensing, Proc. of 3rd Int. Colloq. on Spectral Signatures of Objects in Remote Sens., Les Arcs, France

Goel, N.S., Grier, T. (1988), Estimation of Canopy Parameters for Inhomogeneous Vegetation Canopies from Reflectance Data: III. TRIM: A Model for Radiative Transfer in Heterogeneous Three-Dimensional Canopies, *Remote Sen. of Environ.*, 25:255-293

Goetz A., Rock, B., and Rowan, L. (1983), Remote Sensing for Exploration: An Overview, *Econ. Geol.*, 78, 573-590

Goward, S.N., and Huemmrich, K. F. (1990), Remote sensing of the absorption of photosynthetically active radiation by vegetation canopies, In: 1990 International Geoscience and Remote Sensing Symposium, IEEE, pp. 1213-1216, University of Maryland, College Park, Maryland

Goward, S.N., and Huemmrich, K. F. (1992), Vegetation canopy PAR absorptance and the normalized difference vegetation index: an assessment using the SAIL model, *Remote Sens. Environ.*, 39:119-140

Hall, F. G., Huemmrich, K. F., and Goward, S. N. (1990), Use of narrow band spectra to estimate fraction of absorbed photosynthetically active radiation, *Remote Sens. Environ.*, 32:47-54

Hardwick, K. and Baker, N. R. (1973), *In vivo* measurement of chlorophyll content of leaves, *New Phytol.*, 72:51-54

Hatfield, J. L., Asrar, G., Kanemasu, E. T. (1984), Intercepted Photosynthetically Active Radiation Estimated by Spectral Reflectance, *Remote Sens. of Environ.*, 14:65-75

Hielkema, J. U., Roffey, J., Tucker, C. J. (1986), Assessment of ecological conditions associated with the 1980/81 desert locust plague upsurge in the West Africa using environmental satellite data, *Int. J. Remote Sensing*, vol. 7, no 11, 1609-1622

Hiscox, J.D., and Isrelstam, G.F., (1979), A Method for the Extraction of Chlorophyll From Leaf Tissue Without Maceration, *Can. J. Bot.*, 57, 1332-1334

Horler, D.N.H., Barber, J., Barringer, A.R., (1980), Effects of Heavy Metals on the Absorption and Reflectance Spectra of Plants, *Inl. J. Remote Sensing.*, 1, 121-136, 1980.

Horler, D.N.H., Dockray, M., and Barber, J. (1983a), The Red Edge of Plant Leaf Reflectance, *Int. J. Remote Sensing*, 4, 273-288

Horler, D.N.H., Dockray, M., Barber, J., and Barringer, A.R. (1983b), Red Edge Measurements for Remotely Sensing Plant Chlorophyll Content, *Adv. Space Res.*, 3, 273-277

Huete, A.R., Jackson, R.D., and POST, D.F. (1985), Spectral response of a plant canopy with different soil backgrounds, *Remote Sens. Environ.*, 17:37-53

Huete, A.R. (1988), A soil adjusted vegetation index (SAVI), *Remote Sens. Environ.*, 25:295-309

Huete, A.R. (1989), Soil influences in remotely sensed vegetation-canopy spectra. Theory and Applications of Optical Remote Sensing (G. Asrar, Ed), New York, Wiley, pp 107-141

Kimes, D.S., (1984), Modeling the directional reflectance from complete homogeneous vegetation canopies with various leaf-orientation distributions. *J. Opt. Soc. Amer.*, 1:725-737

Kumar, M. and Monteith, J. L. (1981), Remote sensing of crop growth. Plants in the Daylight Spectrum. (H. Smith, Ed), New York, Academic Press, pp. 134-144

Larsen, (1980), The boreal forest ecosystem, Academic Press, New York, N.Y.

Leckie, D.G. and Teillet, P.M., Ostaff, D.P. Fedosejevs, G. (1988) Sensor Band Selection for Detecting Current Defoliation Caused by the Spruce Budworm, *Remote Sens.of Environ.*, 26:31-50

Lichtenthaler, H.K. (1987), Chlorophylls and Carotenoids: Pigments of Photosynthetic Membranes, in Methods in Enzymology, vol 148, 350-382, Academic Press, N.Y.

Lieth, H. (1975), Primary production of the major vegetation units of the world, *Ecological Studies*, 14, pp:203-215

Lo, C.P. (1986), Applied remote sensing, Longman Scientific & technical, U.K.

Meek, D.W., Hatfield, J.L., Howell, T.A., Idso, S.B., Reginato, R.J. (1984), A Generalized Relationship Between Photosynthetically Active Radiation and Solar Radiation, *Agron. J.*, Vol. 76, November-December

Miller, J.R., Hare, E.W., Neville, R.A., Gauthier, McColl, W.D., Till, S.M., (1985) Correlation of Metal Concentration with Anomalies in Narrow Band Multispectral Imagery of the Vegetation Red Reflectance Edge, Int. Symp. on Remote Sens. for Exploration Geology, San Francisco

Paltridge, G.W., Barber, J., (1988), Monitoring Grassland Dryness and Fire Potential in Australia with NOAA/AVHRR data, *Remote Sens. Environ.*, 25:381-394

Perry, C.R. Jr., Lautenschlager, L.F. (1984), Functional Equivalence of Spectral Vegetation Indices, *Remote Sens. Environ.*, 14:169-182

Reeve, R.G., Anson, A., Laden, D., (1975), Manual of Remote Sensing, *American Soc. of Photogram.*, pp. 1-50

Richards, J.A. (1986), Remote sensing digital image analysis: An introduction, Springer- Verlag, New York, Chapter 1

Richardson, A.J., and Wiegand, C.L. (1977), Distinguishing vegetation from soil background information, *Photogramm. Eng. Remote Sens.*, 43:1541-1552

Rock, B.N., Hoshizaki, T., and Miller, J.R. (1988), Comparison of In Situ and Airborne Spectral Measurements of the Blue Shift Associated with Forest Decline, *Remote Sens. Environ.*, 24, 109-127

Rock, B.N., Hoshizaki, T., Lichtenthaler, H. and Schmuck, G. (1986), Comparison of in situ Measurements of Forest Decline Symptoms in Vermont (USA) and the Schwarzwald (FRG), Proc. of IGARSS' 86 Symp., Zurich

Rock, B.N., Vogelmann, J.E., Williams, D.L., Vogelmann, A.F., and Hoshizaki, T. (1986), Remote Detection of Forest Damage, *Bioscience*, 7, 439-445

Rosenthal, W.D., Arkin, G.F., Howel, T.A. (1985), Transmitted and Absorbed Photosynthetically Active Radiation in Grain Sorghum, *Agron. J.* 77:841-845

Rouse, J.W., Haas, R.H., Schell, J.A., Deering, D.W., and Harlan, J.C. (1974), Monitoring the vernal advancement of natural vegetation, NASA/GSFC Final Report, Greenbelt, MD

Sellers P.J. (1985), Canopy reflectance, photosynthesis, and transpiration, *International Journal of Remote Sensing*, Vol.6, no.8, 1335-1372

Strahler, A.N., Strahler, A.H. (1978) Mordern Physical Geography, John Wiley & Sons, Chapter 1

Strang, G. (1980), Linear algebra and its applications: second edition, Harcourt Brace Jovanopvich, pp. 107

Suits, G. H. (1972), The calculation of the directional reflectance of a vegetative canopy, *Remote Sens. Environ.*, 2:117-125

Tucker, C. J., Miller, L. D., Pearson, R. L. (1975), Shortgrass prairie spectral measurements, *Photogram. Eng. Remote Sensing*, 41:1157-1162

Tucker, C. J. (1979), Red and photographic infraed linear combinations for monitoring vegetation, *Remote Sens. Environ.*, 8:127-150

Tucker, C.J., Holben, B.H., Elgin, J.H., McMurtrey, J.E. (1981), Remote Sensing of Total Dry Matter Accumulation in Winter Wheat, *Remote Sen. Environ*, 11:171- 189

Tucker, C.J., Miller, L.D. (1977), Soil Spectra Contributions to Grass Canopy Spectral Reflectance, *Photogram. Eng. and Remote Sens.*, Vol. 43, No. 6, pp 721-726.

Venkateswarlu, B., Vergara, B.S., Visperas, R.M. (1987), Influence of Photosynthetically Active Radiation on Grain Density of Rice, *Crop. Sci.*, 27:1210-1214

Verhoef, W. (1984), Light scattering by leaf layers with application to canopy reflectance modeling: the SAIL model, *Remote Sens. Environ.*, 16:125-141

Westman, W.E., and Price, C.V. (1987), Remote Detection of Air Pollution Stress to Vegetation: Laboratory Level Studies, Proc.Int. Geosci. Remote Sens. Symp. (IGARR'87), Ann Arbor, Michigan, pp. 451-456

Westman, C.A., Aber, J.D., Peterson, D.L., and Melillo, J.M. (1988), Foliar analysis using near infred reflectance spectroscopy, *Can. J. For. Res.*, 18:6-11

Williams, D.L. (1989), The radiative transfer characteristics of spruce (picea spp): Implications relative to the canopy micriclimate, The University of Maryland, Ph.D. diss., Biogeography

Woodward, F.I. (1987), Climate & plant distribution, Cambridge University Press, Cambridge, U.K.

Yoder, B., and Daley, L. (1990), Development of a visible spectroscopic method for determining chlorophyll a and b *In vivo* in leaf samples, *Spectroscopy*, Vol.5, No. 8:44-50

Yoder, B.J. (1992), Photosynthesis of conifers: Influential factors and potential for remote sensing, The Oregon State University, Ph.D. Diss., Forest Science, Plant Physiology